Received: 13 September 2024 | Revised: 24 February 2025 | Accepted: 25 February 2025

DOI: 10.1111/joa.14243

Journal of Anatomy | ANATOMICAL SOCIETY WILEY

ORIGINAL ARTICLE

Locomotor signals in the trabecular structure of the hominoid clavicle

Hannah N. Farrell | Rena Schwartz | Zewdi J. Tsegai | Zeresenay Alemseged

Department of Organismal Biology and Anatomy, The University of Chicago, Chicago, Illinois, USA

Correspondence
Hannah N. Farrell, Department of Organismal Biology and Anatomy, The University of Chicago, Chicago, Illinois, USA.
Email: hannahh.farrell@gmail.com

Funding information
Leakey Foundation; NSF Social, Behavioral, and Economic Sciences (SBE) Division, Grant/Award Number: DDRIG-BA 2317012; University of Chicago, Hinds Foundation

Abstract

Understanding the functional significance of morphological variation is crucial for investigating locomotor adaptations in fossil primates and early hominins. However, the nuanced form–function relationship in the upper limbs of extant apes is difficult to discern due to their varied locomotor behaviors, complicating the interpretation of similar features in fossil hominins. Trabecular bone, which responds to mechanical strain, reflects the intensity and direction of forces during movement, making it valuable for identifying locomotor adaptations in hominoids. This study examines trabecular bone in the clavicle—a crucial component of shoulder biomechanics—to explore its relationship to mechanical loading patterns and bone functional adaptations in primate locomotion. Using a whole-bone approach, we analyzed trabecular structure in the clavicle of apes: *Gorilla* spp. (*G. beringei*: $N = 28$; *G. gorilla*: $N = 29$), *Homo sapiens* ($N = 19$), *Hylobates* spp. (*H. lar*: $N = 28$; *H. concolor*: $N = 3$), *Pongo* spp. (*P. abelii*: $N = 13$; *P. pygmaeus*: $N = 24$), and *Pan troglodytes* ($N = 35$), quantifying relative bone volume fraction (rBV/TV), trabecular thickness (Tb.Th), trabecular separation (Tb.Sp), and trabecular number (Tb.N) from high-resolution micro-CT scans. Aspects of the clavicular trabecular architecture among ape taxa appear to correspond to differences in locomotor behavior. In most taxa, rBV/TV is highest in regions underlying muscle attachment sites frequently used during upper limb activities, with differences among taxa predominantly reflecting variations in upper limb use and muscle attachment sites. Regions of high rBV/TV beneath entheses and articular surfaces result from different trabecular parameters—higher rBV/TV is achieved primarily via greater Tb.Th under entheses, while in subarticular regions, it is driven by higher Tb.N. However, no consistent differences in sternoclavicular subarticular trabecular bone emerge between *Homo* and the other apes, despite differences in shoulder positioning on the torso. Muscle activity appears to significantly influence trabecular bone structure in the clavicle of living apes, with implications for reconstructing early hominin locomotor behaviors and upper limb use.

KEYWORDS
BV/TV, clavicle, hominoid, locomotion, trabecular bone

1 | INTRODUCTION

To effectively test hypotheses about the locomotor adaptations of early hominins, a detailed understanding of the form–function relationship in the pectoral girdle of extant apes is essential. The functional morphology of the hominoid upper limb has been extensively explored, aiming to reconstruct both early hominin behaviors (Arias-Martorell et al., 2015; Drapeau, 2004; Larson, 2013; Marzke, 1983; Rein, 2019; Susman et al., 1984; Ward, 2013), and characteristics of the most recent common ancestor of *Pan* and *Homo* (Almécija et al., 2021; Crompton et al., 2008; Thorpe et al., 2007; White et al., 2015; Young et al., 2015). Nevertheless, despite this breadth of research and a range of methodological approaches, conflicting interpretations of the same traits continue to obscure our understanding of the relationship between ape shoulder morphology and biomechanical function.

Exploring the plasticity of bony morphology may help resolve these ongoing issues and bring clarity to current debates. Research on the elements in the upper limb has already demonstrated the potential of investigating developmental plasticity (Barros, 2014; Cowgill, 2007; Green, 2013; Green & Alemseged, 2012) and internal bone structure (Bird et al., 2022; Dunmore et al., 2023; Kivell et al., 2018; Skinner et al., 2015; Tsegai et al., 2013) to deepen our understanding of the form-function relationship in hominins. For example, the juvenile *Au. afarensis* DIK-1-1 scapula suggests that the shoulder of *Au. afarensis* developed along a trajectory more similar to extant African apes than to modern humans, emphasizing the species' reliance on arboreal behaviors (Green & Alemseged, 2012). Moreover, humeral torsion has been shown to be developmentally plastic in modern humans (Cowgill, 2007) and extant hominoids (Barros, 2014), underscoring its significance as a functional trait in fossil hominins (Larson, 2013). In contrast, clavicular morphology appears to be developmentally static, showing little external plasticity (Corrigan, 1960; Farrell, 2024). Given the limitations of phylogenetic relatedness, which can restrict morphological variation through genetic factors, and anatomical constraints, such as the need for joint congruence, on external morphology (Lieberman et al., 2001; Ruff & Runestad, 1992), understanding hominin shoulder adaptations may benefit from examining plastic morphological features, such as internal bone structures (Kivell, 2016; Ruff et al., 2006; Ward, 2002).

Trabecular bone, which adapts in response to strain during an organism's lifetime (Ehrlich & Lanyon, 2002; Eriksen, 1986; Eriksen, 2010), can offer valuable insights into the mechanical loading history of a bone, including how forces are distributed across the joint surface (Dunmore et al., 2020; Kivell et al., 2018; Tsegai et al., 2013) and their orientation (Barak et al., 2011; Barak et al., 2013; Huiskes et al., 2000). In comparison to external morphological traits, trabecular bone is thought to be more responsive to stress and strain compared to external aspects of morphology and therefore may better reflect the behaviors an animal was engaged in as opposed to the full range of possible behaviors with a given joint or element configuration (Ruff & Runestad, 1992). Even in comparison to cortical bone, which remodels at a rate of about 2%–3% per year, trabecular bone generally remodels much faster, with approximately 25% turnover annually in healthy adults (Eriksen, 1986, Eriksen, 2010); although, the exact remodeling rate likely varies both phylogenetically (Currey et al., 2017; Wallace et al., 2012; Wallace, Judex, & Demes, 2015), through ontogeny (Pitfield et al., 2017; Wallace, Demes, & Judex, 2017), and even regionally within the same skeletal element (Parfitt, 2002; Wallace et al., 2017; Wallace, Pagnotti, et al., 2015). With such a high turnover rate, trabecular bone is thought to be more responsive to variation in mechanical loading throughout life and therefore may better reflect function than cortical bone (Carter et al., 1989; Jacobs, 2000; Rubin et al., 2001, 2002; but see Lovejoy et al., 2003). Additionally, the trabecular response to loading appears to be more localized than that of cortical bone (Barak et al., 2011; Judex et al., 2004; Rubin et al., 2001; Rubin et al., 2002; Schulte et al., 2013), potentially allowing for the identification of more nuanced signals of locomotor adaptation.

The architecture of primate trabecular bone, particularly in load-bearing joints, has been shown to reflect mechanical demands, offering valuable insight into variation in locomotor strategies. In metacarpals, trabecular bone volume fraction (BV/TV) varies with joint loading, with regions of high BV/TV indicating areas of habitual compressive loading, offering insight into joint posture during locomotion and distinguishing suspensory from knuckle-walking primates (Chirchir et al., 2017; Dunmore et al., 2020; Dunmore et al., 2023; Tsegai et al., 2013). Subarticular trabecular bone in the femoral and humeral heads has similarly been used to distinguish locomotor groups among anthropoids (Georgiou et al., 2019; Ryan & Shaw, 2012). In particular, BV/TV underlying the subarticular surface of the femoral head correlates with hip posture and loading across the locomotor regimes of humans and African apes, with humans displaying a single region of high BV/TV reflecting bipedal walking, while *Pan* and *Gorilla* show two regions corresponding to climbing and knuckle-walking (Georgiou et al., 2019). Additionally, features such as trabecular number, connectivity density, and fabric anisotropy in the center of the femoral, and to a lesser extent humeral head, analyzed together appear to distinguish among locomotor modes in anthropoids (Ryan & Shaw, 2012). However, the relationship between trabecular structure and function is not consistent across all elements. Studies of the talus, for example, reveal significant overlap in trabecular patterns among hominoids with different locomotor behaviors, suggesting that this element does not simply reflect locomotor loading (DeSilva & Devlin, 2012). Similarly, trabecular structure in the humeral head overlaps among hominoids, likely due to shared arboreal behaviors, complicating its effectiveness in distinguishing among locomotor strategies (Kivell et al., 2018). Broader studies of trabecular architecture across the skeleton reveal systemic patterns that are not always tied to locomotor differences. Chimpanzees, for instance, generally have slightly higher BV/TV than humans in most regions (Tsegai et al., 2018), and in modern humans, the cervical vertebrae, proximal femur, and proximal humerus consistently exhibit the highest BV/TV (Ryan et al., 2019), indicating that trabecular variations often reflect other factors beyond locomotion.

Traditionally, analyses of trabecular adaptation have concentrated on the areas underlying joint surfaces, where trabecular bone is thought to manage and distribute loads to the surrounding cortical bone (Barak et al., 2008; Currey, 2002). However, in some bones, like the clavicle, trabecular structure extends beyond these joint regions and plays a role throughout the diaphysis. This extended presence suggests that trabecular bone may have additional functions, such as supporting diaphyseal stiffness under regular loading or serving non-mechanical roles such as facilitating hematopoiesis, as observed in humans (Keaveny et al., 2001; Wang et al., 2022; Zawin and Jaramillo, 1993). Given that about 88% of trabecular stiffness, or the Young's modulus of trabecular bone, can be explained by BV/TV (Stauber et al., 2006), regions of the diaphysis with increased BV/TV may be specifically adapted to resist the stresses imposed during locomotion. Moreover, entheses—the regions where tendons and ligaments attach to bone (Benjamin & McGonagle, 2009)—are commonly found along the diaphyses of long bones and are subject to significant tensile forces transmitted through these connective tissues (Benjamin et al., 2008; Benjamin & Ralphs, 1997). Since bones are more susceptible to failure under tensile loading compared to compression (Doube et al., 2009; Pattin et al., 1996), the trabecular and/or cortical bone underlying these entheses would be expected to exhibit adaptations, such as higher bone volume fraction (BV/TV). However, studies of cortical geometry in the hominoid clavicle suggest that its morphology is more strongly influenced by bending loads on the bone as a whole, rather than localized signals from muscle action (Farrell, 2024; Farrell and Alemseged, 2025). Thus, while cortical bone may contribute to reinforcing areas of high mechanical demand, in the hominoid clavicle, the trabecular bone underlying entheses is still likely to exhibit elevated BV/TV to accommodate localized tensile stresses. This increased density would help to accommodate the concentrated forces from muscle contractions, thereby enhancing the bone's structural integrity in response to repetitive, localized stress (Benjamin & Ralphs, 1997; Schlecht, 2012).

In addition to focusing on more functionally informative aspects of morphology, incorporating the clavicle into analyses alongside the scapula and humerus could help address the challenges in identifying consistent functional signals in the pectoral girdle. The hominoid clavicle, often understudied compared to these other elements, is particularly well-suited for studying bone functional adaptation due to its unique properties and roles. In primates, the clavicle acts as the only bony articulation between the thorax and upper limb (Harrington et al., 1993; Ljunggren, 1979). Relative to the soft tissues around it, the clavicle has the highest Young's modulus (Gordon, 2009), making it the most rigid structure for transferring loads between the substrate and the body of the locomoting animal. Moreover, analysis of cortical geometry suggests that the clavicle, bridging the upper limb and thorax, experiences varied loading patterns during different locomotor behaviors (Farrell, 2024; Farrell and Alemseged, 2025). Finally, the average primate clavicular diaphysis serves as an attachment site for three muscles crucial for upper limb flexion and abduction during locomotion: the clavicular head of the pectoralis major muscle along its sternal ventral surface (except in *Pongo*), the anterior deltoid muscle (clavicular head) on the cranioventral surface of the lateral third of the bone, and the cranial trapezius muscle along the craniodorsal surface of the same region (Diogo & Wood, 2012; Swindler & Wood, 1973). Alongside these muscular attachments, the presence of trabecular bone throughout the clavicular diaphysis (Harrington et al., 1993) makes it particularly suited for studying the structural role of trabecular bone beyond the subarticular regions.

Here, we examine whether the trabecular bone structure in the clavicle varies predictably between hominoids to understand the patterns of biomechanical loading imposed by differing locomotor practices. To explore these variations, we test several hypotheses: (1) suspensory taxa (*Pongo*, *Hylobates*) will exhibit decreased BV/TV in the central subarticular regions of the clavicle due to tensile joint loading and increased BV/TV at the periphery reflecting tensile forces at ligamentous attachments, while more terrestrial taxa (*Pan*, *Gorilla*) will have higher BV/TV throughout the subarticular regions, reflecting compressive joint loading; (2) regions of attachment for the clavicular pectoralis major m., anterior deltoid m., and cranial trapezius m. will have higher BV/TV than areas of the diaphysis devoid of muscle and/or ligament attachment (Figure 1; Doube et al., 2009; Pattin et al., 1996); (3) Tb.N will be highest, and BV/TV and Tb.Th will be lowest in the smallest non-human apes (*Hylobates*, *Pan*) and greatest in the larger non-human apes (*Gorilla*, *Pongo*), reflecting the scaling relationship reported in analyses of other skeletal elements (Doube et al., 2011; Ryan & Shaw, 2013); and (4) modern *Homo sapiens* will have the lowest relative BV/TV among the great apes, reflecting the recent gracilization of the modern human skeleton noted by other researchers (Chirchir et al., 2015; Ruff, 2006; Ryan & Shaw, 2015).

2 | MATERIALS AND METHODS

2.1 | Materials

Trabecular bone parameters were measured from microcomputed tomographic (micro-CT) scans of the clavicle in a sample of wild-origin adult apes (*Homo sapiens*, $N = 20$; *Gorilla gorilla*, $N = 32$; *Gorilla beringei*, $N = 16$; Pan troglodytes, $N = 34$; Pongo abelii, $N = 13$; Pongo pygmaeus, $N = 24$; Hylobates lar, $N = 28$; and Hylobates concolor, $N = 3$; Table 1; Table S1). To enable generic comparisons, both species of *Gorilla* were combined, as were both species of *Pongo* and *Hylobates*. The extant ape sample includes specimens housed in the American Museum of Natural History (AMNH), Cleveland Museum of Natural History (CMNH), Field Museum of Natural History (FMNH), Harvard Museum of Comparative Zoology (MCZ), Max Planck Institute for Evolutionary Anthropology (MPI), and Smithsonian Institution (USNM, formerly National Museum of Natural History). The modern *Homo*

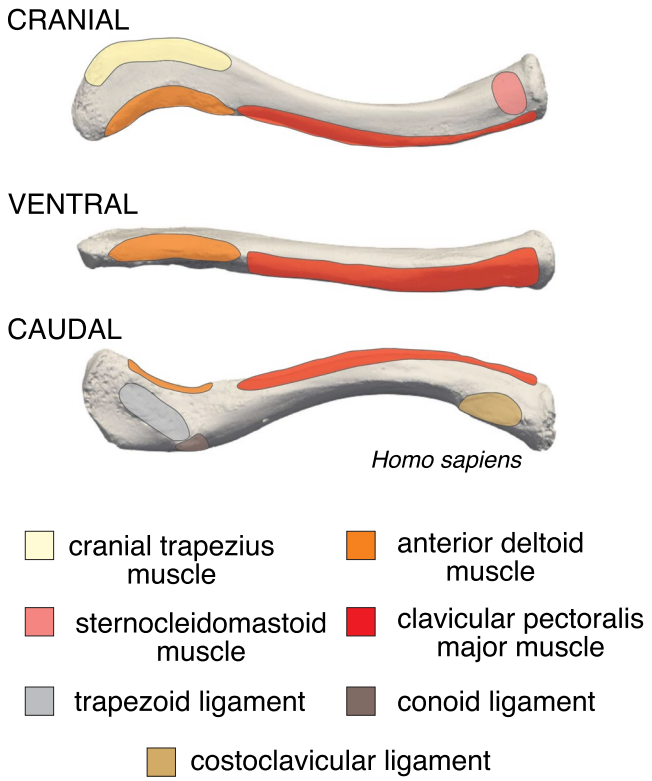

FIGURE 1 Attachment sites of the cranial trapezius muscle (pale yellow), anterior deltoid muscle (orange), clavicular pectoralis major muscle (red), sternocleidomastoid muscle (pink), trapezoiz ligament (grey), conoid ligament (brown), and costoclavicular ligament (gold) on a modern *Homo sapiens* clavicle, as seen in cranial view (top) and ventral view (bottom). Minor variations in muscle attachment do exist among the apes, for example, the trapezius attaches to "more than the lateral third" of the clavicle in *Hylobates*, compared to "the lateral third or more than the lateral third" in *Pan*. Most notably, *Pongo* does not have a clavicular origination of the clavicular pectoralis major muscle (see Diogo & Wood, 2011, 2012).

TABLE 1 Extant adult hominoid sample.

Genus	N_{total}	M	F	U
Gorilla spp.	48	29	18	1
Homo sapiens	20	10	10	0
Hylobates spp.	31	16	14	1
Pan troglodytes	34	20	14	0
Pongo spp.	37	15	22	0

Note: Sex is indicated as M (male), F (female), or U (unknown). Detailed specimen information and micro-CT scanning parameters are available in the Supplemental Information.

sapiens sample is sourced from the Hamann-Todd Collection and includes post-industrial individuals of known age and sex. Non-pathological right clavicles, free from evidence of mounting, were preferentially sampled. Left clavicles were occasionally sampled when the right one was missing or damaged but were mirrored prior to conducting analyses. Individuals were determined to be adults based on the presence of all three permanent maxillary and mandibular molars (Smith et al., 1994) alongside the fusion of the sternal clavicular epiphysis. To minimize the effects of sexual dimorphism, adult females and males were sampled proportionally when possible.

Micro-CT scans of the extant individuals were generated at the University of Chicago using a Phoenix|x-ray Nanotom and v|tome|x combination (RRID:SCR_024763), the Center for Nanoscale Systems at Harvard University using an HMXST Micro-CT x-ray imaging system, and the Max Planck Institute for Evolutionary Anthropology using a diondo d3. Due to the variation in specimen size and density, voltage ranged from 70 to 110 kV, current ranged from 150 to 320 μA, resolution ranged from 27.38 to 89.20 μm and either no filter or a 0.2 or 0.5 mm copper filter was used. While some of the larger great apes were scanned at a lower resolution, the average trabecular thickness in these specimens exceeds 0.1 mm (100 μm), ensuring that the resolution remains sufficient for accurate measurements (also see Lukova et al., 2024). Detailed specimen information and CT scan parameters are provided in Table S1 within the Supplementary Material.

2.2 | Methods

2.2.1 | Segmentation and reorientation

The micro-CT data was first segmented using the MIA-Clustering segmentation algorithm (Dunmore et al., 2018) to reduce the number of subjective decisions and increase reproducibility. The resulting segmented scans were first manually inspected to confirm the accuracy of the segmentation. Next, the scans were binarized and reoriented into standardized anatomical positions using *Avizo Lite 2020.2* (Visualizations Sciences Group, 2017), with the *x*-axis representing the dorsoventral plane, the *y*-axis representing the craniocaudal plane, and the long axis of the clavicle aligned with the *z*-axis, ensuring that all specimens were in the same position when defining the regions of interest (ROIs; Figure 2a).

Using medtool (v 4.5; www.dr-pahr.at/medtool), the cortical and trabecular bone were differentiated using morphological filters with an in-house script following Gross et al. (2014). Briefly, first a closing filter was used to fill in any gaps in the cortex of the element. After the surface was closed, an outer and inner mask of the element were created, representing the periosteal and endosteal volumes of the specimens. A cortex-only mask was then created by subtracting the inner mask from the outer mask, and a trabecular bone-only mask was created by subtracting the cortical image from the full original image. The created masks were then mathematically combined such that the cortex was removed, and the air, inner medullary region, and trabecular bone in the image are assigned the grey values 0, 1, and 2, respectively (Figure 2a); this defined voxel data was used to quantify the trabecular parameters of interest. A volumetric mesh of the inner mask was created, upon which the quantified trabecular parameters were interpolated (Figure 2c).

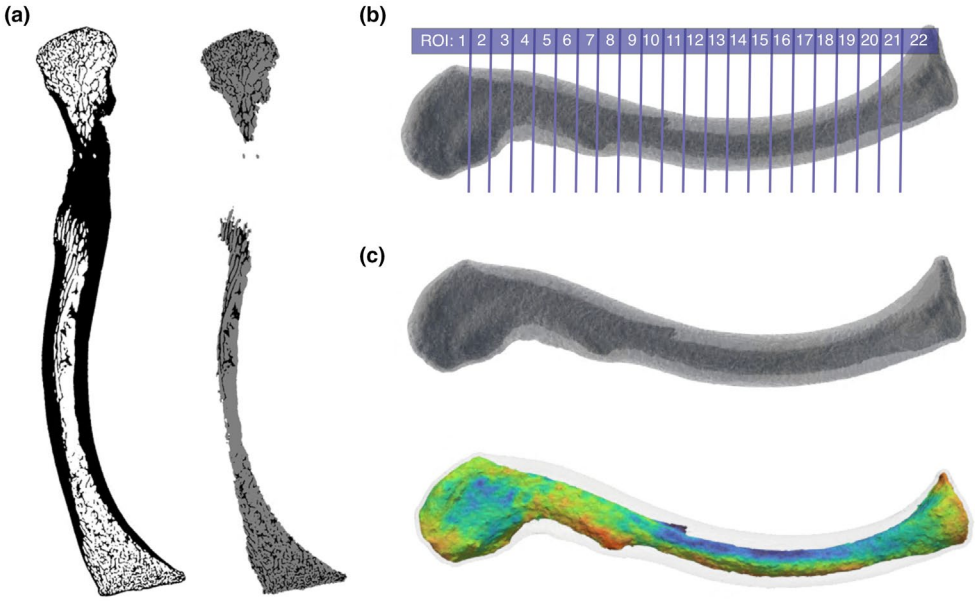

FIGURE 2 Processing stages for analysis of trabecular bone structure, shown here in a modern *Homo sapiens* clavicle: (a) mid-plane image of the binarized and aligned bone (left) and final masked image (right); (b) the 22 ROIs used for statistical comparison; (c) 3D finite element meshes created from the outer and inner masks upon which the whole-bone data will be projected (top) and the interpolated values used to produce a 3D morphometric map of BV/TV with warmer tones indicating higher BV/TV and cooler tones indicating lower BV/TV (bottom).

2.2.2 | Trabecular bone quantification

First, comprehensive trabecular bone mapping was conducted across the entire clavicle to visualize the parameters throughout the element. To achieve this, a 2.5 mm square grid was overlaid onto the mesh representing the endosteal volume of the specimen. A 5 mm sampling sphere was then fitted to each node in the grid, resulting in many overlapping spheres. Within each of those spheres, trabecular bone volume fraction (BV/TV) was quantified. These BV/TV values were then interpolated onto the endosteal mesh, providing a global visualization of BV/TV.

Next, BV/TV, trabecular thickness (Tb.Th), trabecular separation (Tb.Sp), and trabecular number (Tb.N) were quantified within predefined 3D ROIs to enable statistical comparisons. Specifically, this means that BV/TV was calculated both globally for the entire clavicle (as described above) and locally for each of the ROIs. ROI 1 quantified the sternal subarticular area (medial 10% of bone length), ROI 22 quantified the acromial subarticular area (lateral 10% of bone length), and the intermediate 20 regions (ROI 2 – ROI 21) each quantified 4% of bone length, collectively covering the remaining 80% of bone (Figure 2b).

Within medtool, BV/TV is calculated as the ratio of 'BV' or bone volume (all voxels with a '2' grey value) over 'TV' or total volume (all voxels with a '1' and '2' grey value). Tb.Th and Tb.Sp were calculated using the sphere fitting method of Hildebrand and Ruesegger (1997), and Tb.N was calculated as 1 divided by the sum of Tb.Th and separation (1/(Tb.Th + Tb.Sp)). To control for potential systemic differences in mean BV/TV across specimens and to allow for a more meaningful exploration of relative patterns, BV/TV was standardized by dividing the original values by the mean BV/TV for each individual specimen, resulting in the relative trabecular bone volume fraction (rBV/TV; Dunmore et al. 2020).

2.2.3 | Comparative analyses

To qualitatively compare the distributions of the parameters across the clavicle, values calculated for those parameters at each node in the grid during the whole bone analysis were projected onto the nodes of the 3D mesh (Figure 2c). The interpolation of these values and projection onto the 3D mesh were visualized in *Paraview 5.11.0* (Ahrens et al., 2005). To better understand the regional variation in trabecular bone structure, this visualization was performed and described for the specimen with BV/TV values in each ROI closest to the genus average (*Gorilla*, AMNH M 167336; *Homo*, CMNH HTH 0315; *Hylobates*, MCZ M 41455; *Pan*, AMNH M 174860; *Pongo*, USNM M 143596).

2.2.4 | Statistical analysis

Statistical comparison of the structural parameters was conducted using the mean rBV/TV, Tb.Th, Tb.Sp, and Tb.N values for each of the 22 defined ROIs. Levene's tests were used to assess for significant differences in homogeneity of variance between groups, and Shapiro–Wilk tests were used to identify datasets that deviated from a normal distribution. Fifty-six of the defined groups showed differences in homogeneity of variance ($p < 0.00001$ to $p = 0.85$), and 94 had non-normal distributions ($p < 0.00001$ to $p = 0.63$), so further differences between groups were investigated with non-parametric

Kruskal–Wallis tests and post hoc Dunn's tests with Bonferroni correction to control the family-wise error rate. Adjusted *p*-values (*p.adjust*) are reported and range from $p < 0.00001$ to $p = 1$ (Tables S2–S6). Since certain trabecular parameters have been shown to scale allometrically with body mass (Cotter et al., 2009; Doube et al., 2011; Plasse et al., 2019; Ryan & Shaw, 2013; Smith et al., 2024; Swartz et al., 1998), we explored our data for similar allometric relationships. Mean values for BV/TV, Tb.Th, Tb.Sp, and Tb.N were calculated for each individual and subjected to an ordinary least squares linear regression using clavicle length, which scales relatively isometrically with body mass in primates (Kagaya et al., 2010; Laudicina & Cartmill, 2023; Niskanen & Junno, 2009), as a proxy for body mass (Table 2) to assess how these trabecular parameters in the clavicle scale with variations in body size. As both Tb.Th and Tb.Sp are linear size variables, a slope (β) of 1 would indicate isometry, with slopes above 1 indicating positive allometry and those below 1 indicating negative allometry. In contrast, because BV/TV and Tb.N are shape variables, a slope (β) of 0 would indicate isometry, with positive values indicating positive allometry and negative values indicating negative allometry. All statistical analyses were carried out in R 4.3.2 (R Core Team, 2023), with statistical significance thresholds set at $p.adjust = 0.05$ for the Kruskal–Wallis and Dunn tests and $p = 0.05$ for the tests of allometry.

3 | RESULTS

3.1 | Trabecular bone volume fraction (BV/TV and rBV/TV)

The initial analysis of BV/TV reveals significant differences among hominoid taxa (Figure 3a; Table S2). *Hylobates* is notably distinct from the great apes, exhibiting substantially lower BV/TV across the entire diaphysis. Among the great apes, *Homo* displays lower BV/TV at the acromial end compared to *Gorilla*, *Pan*, and *Pongo*, although sternal values are similar across these taxa. *Gorilla* is distinguished by having higher BV/TV at the acromial end relative to the other great apes, while *Pan* and *Pongo* show similar patterns of BV/TV across the clavicle. Allometrically, BV/TV scales positively with bone length across all apes (slope = 1.347; Table 2), indicating a strong relationship between the two variables. In contrast, no significant allometric relationship is observed within the great apes, suggesting a much weaker association between BV/TV and bone length in this group. Additionally, no significant intraspecific trends in BV/TV were detected across any of the ape species.

Even after normalizing the BV/TV values by individual specimen means (rBV/TV), significant differences persist among hominoid taxa (Figure 3b; Table S3). *Homo* now exhibits higher rBV/TV in the sternal half of the diaphysis compared to *Pan*, *Pongo*, and *Gorilla*. As for unscaled BV/TV, *Hylobates* displays lower rBV/TV than all the great apes between 41% and 75% of bone length. The rBV/TV distributions in *Pan* and *Gorilla* largely overlap, except between 86% and 91% of bone length, where rBV/TV in *Pan* is lower than in *Gorilla* and is more similar to *Homo*. In the same region, the rBV/TV of *Gorilla* aligns more closely with *Pongo*. A general trend across the great apes shows an increase in rBV/TV around 60%–70% of bone length. However, again *Hylobates* presents a distinct distribution, with rBV/

TABLE 2 Ordinary least squares linear regressions of log-transformed mean trabecular parameters against bone length as a proxy for body mass to test for allometric relationships in the dataset.

	F-statistic	Adjusted R^2	β	*p*-value
All Apes				
BV/TV	185.4	0.5308	1.347	**<0.0001**
Tb.Th	160.9	0.4953	0.599	**<0.0001**
Tb.N	9.835	0.0514	0.147	**0.002**
Tb.Sp	30.72	0.1542	−0.405	**<0.0001**
Great Apes				
BV/TV	1.842	0.0063	0.181	0.177
Tb.Th	5.34	0.0318	0.002	**0.031**
Tb.N	13.81	0.0885	−0.274	**0.0003**
Tb.Sp	6.502	0.04001	0.292	**0.012**
Gorilla				
BV/TV	0.539	−0.0104	−0.199	0.468
Tb.Th	0.083	−0.0208	−0.056	0.775
Tb.N	1.742	0.0162	−0.221	0.192
Tb.Sp	3.183	0.0463	0.516	0.081
Homo				
BV/TV	0.179	−0.0507	0.186	0.678
Tb.Th	80.48	0.8238	0.973	**<0.0001**
Tb.N	3.079	0.109	−0.639	0.099
Tb.Sp	1.439	0.0252	0.661	0.248
Hylobates				
BV/TV	2.131	0.0363	1.370	0.155
Tb.Th	3.913	0.0885	0.696	0.058
Tb.N	1.305	0.0101	−0.487	0.263
Tb.Sp	1.095	0.0032	0.593	0.304
Pan				
BV/TV	1.806	0.0246	0.763	0.189
Tb.Th	8.528	0.1905	0.636	**0.0065**
Tb.N	7.446	0.1677	−0.622	**0.0104**
Tb.Sp	1.573	0.0176	0.480	0.219
Pongo				
BV/TV	0.073	−0.0272	0.089	0.789
Tb.Th	0.029	−0.0285	−0.031	0.867
Tb.N	0.027	−0.0286	0.029	0.869
Tb.Sp	0.043	−0.0281	−0.052	0.836

Note: The scaling coefficient (β) represents the slope in allometric analysis. For BV/TV and Tb.N, β = 0 indicates isometry, while for Tb.Th and Tb.Sp, β = 1 indicates isometry. Values above or below these thresholds suggest positive or negative allometry, respectively. Significance was determined at $p = 0.05$, with significant *p*-values bolded.

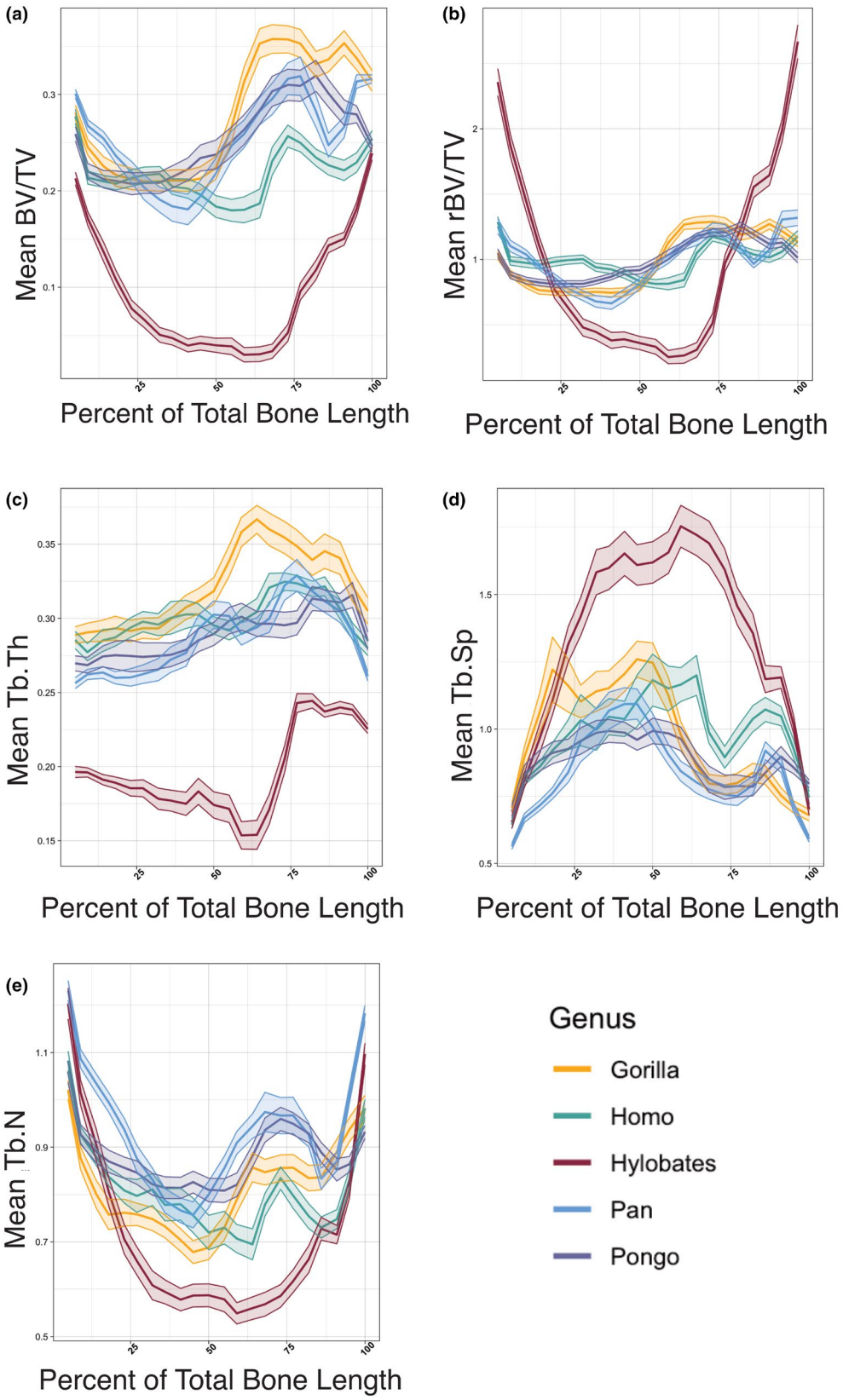

FIGURE 3 Mean trabecular structure parameters along the clavicle of extant apes. The *x*-axis represents the position along the clavicle, with 0 indicating the sternal end and 100 the acromial end. The y-axis displays: (a) unscaled trabecular bone volume fraction (BV/TV), (b) mean relative trabecular bone volume fraction (rBV/TV), (c) trabecular thickness (Tb.Th), (d) trabecular separation (Tb.Sp), and (e) trabecular number (Tb.N). Lines are color-coded by genus and represent the genus-specific means, with shaded regions illustrating the standard error.

TV being highest within the epiphyses and remaining low throughout the diaphysis.

To better understand the regional variation in trabecular bone structure, the distribution of rBV/TV is described in a specimen with BV/TV values closest to the genus mean. These patterns are generally consistent across the sample, though some minor variation is observed. In *Gorilla*, the highest rBV/TV values are observed on the cranial surface of the lateral curvature and at the acromial end (Figure 4). Notably, *Gorilla* shows particularly low rBV/TV values at mid-diaphysis (Figures 4–7). Within the subarticular regions (Figure 8), the sternal area typically exhibits higher rBV/TV at the center of the articular surface, though there is variation, with some cases showing a slightly more cranial placement of this concentration. Conversely, the acromial subarticular area exhibits a relatively even distribution of rBV/TV.

In *Pan*, high rBV/TV values are also concentrated around the lateral curvature (Figure 4); however, the signal extends more medially into the diaphysis than in *Gorilla* (Figures 4–7). Also, unlike *Gorilla*, *Pan* exhibits elevated rBV/TV throughout both the acromial and sternal subarticular regions. Acromially, *Pan* shows consistently high rBV/TV across the entire subarticular area, while sternally, it follows a similar pattern to *Gorilla*, but with a more diffuse spread of high rBV/TV across most of the surface (Figure 8). The specimen shown in Figure 8, however, lacks high BV/TV in the center of the sternal epiphysis, reflecting the trabecular structure typically observed when pitting is present on the sternal articular surface. Additionally, the sternal end of the clavicular diaphysis in *Pan* shows particularly high rBV/TV around the attachment site for the sternocleidomastoid muscle (Figure 4).

Homo exhibits the highest rBV/TV values along the ventral margin of the diaphysis, particularly in the medial aspect at the attachment site for the clavicular head of the pectoralis major muscle (Figure 5). These elevated values extend cranially in the region of the lateral curvature near where the anterior deltoid muscle originates. Slightly elevated rBV/TV is also observed in the region associated with the attachment of the cranial trapezius muscle (Figure 4), although this signal is less pronounced compared to the other described regions. Though variable in the sample, some individuals also show increased rBV/TV in the region of attachment for the sternocleidomastoid muscle on the superior surface of the medial clavicle. A distinct pattern of rBV/TV is observed within the inferior aspect of the lateral curvature: the ventral half exhibits high rBV/TV, while the dorsal half shows markedly lower values (Figure 6). This distribution best resembles the pattern seen in *Gorilla* rather than *Pan* or *Pongo*. Moreover, the dorsal aspect of the diaphysis has generally low rBV/TV values throughout the element (Figure 7). In the

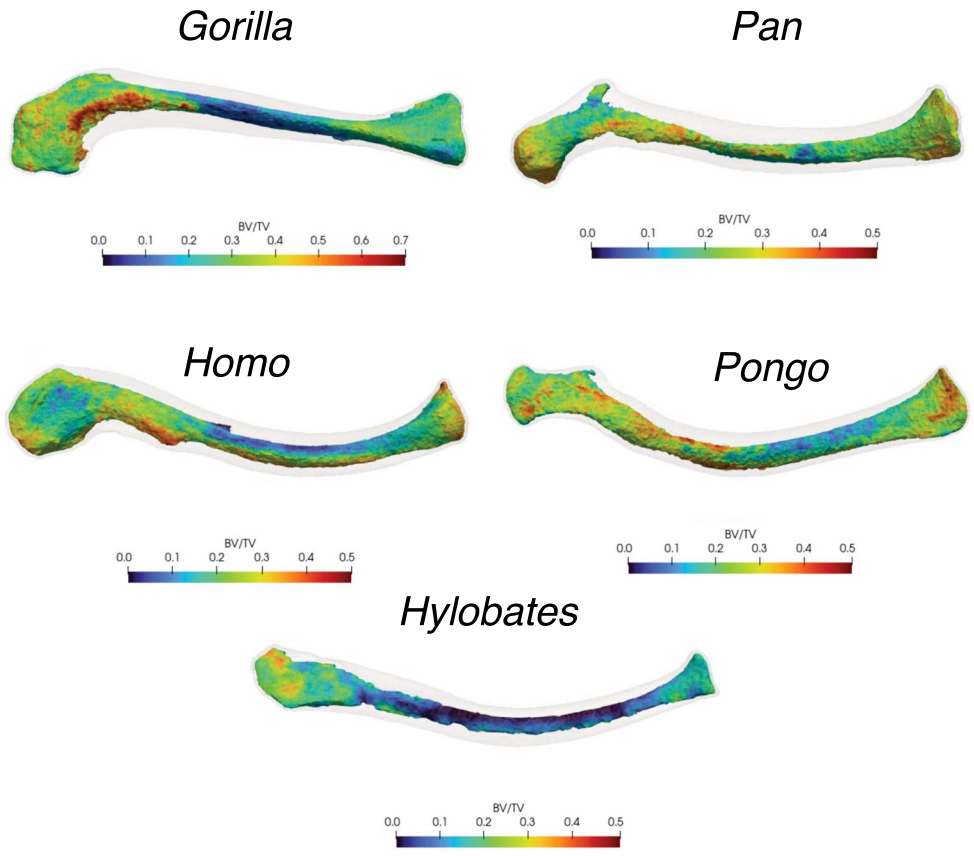

FIGURE 4 Intraspecific variation in BV/TV in the hominoid clavicle. Surface level patterns of BV/TV in cranial view. The color map has been scaled based on the mean ± 3 standard deviations of BV/TV for each specimen, with warmer tones indicating higher BV/TV and cooler tones indicating lower BV/TV. Generic level patterns are represented by the following specimens: *Gorilla* (AMNH M 167336), *Pan* (AMNH M 174860), *Homo* (CMNH HTH 0315), *Pongo* (USNM M 143596), and *Hylobates* (MCZ M 41455).

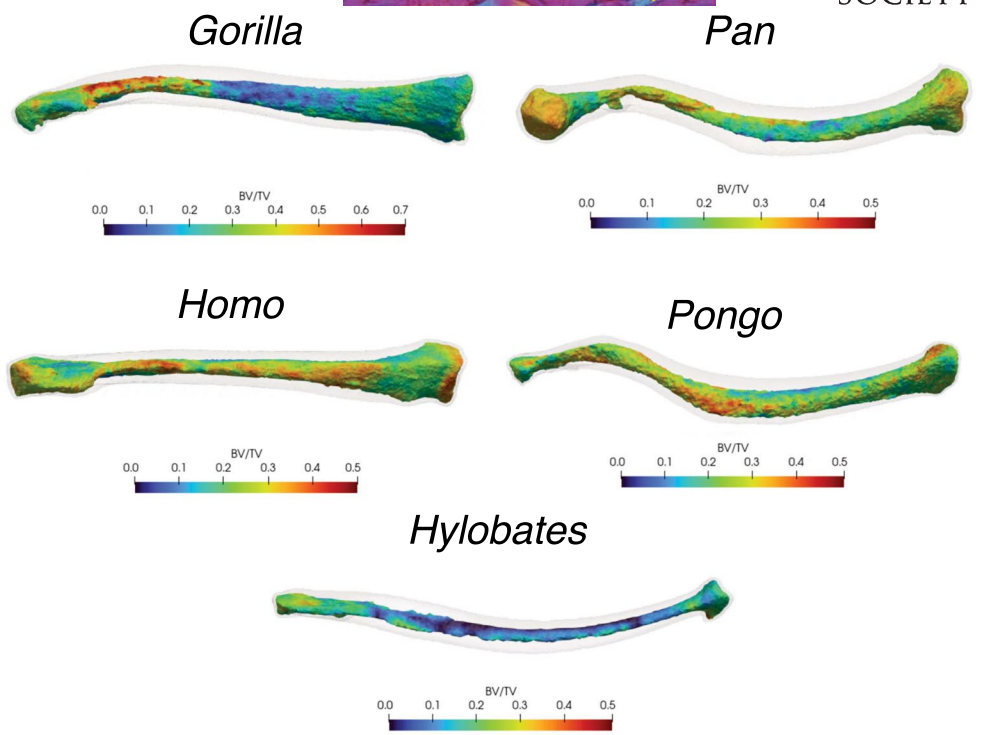

FIGURE 5 Intraspecific variation in BV/TV in the hominoid clavicle. Surface level patterns of BV/TV in ventral view. The color map has been scaled based on the mean ± 3 standard deviations of BV/TV for each specimen, with warmer tones indicating higher BV/TV and cooler tones indicating lower BV/TV. Generic level patterns are represented by the following specimens: *Gorilla* (AMNH M 167336), *Pan* (AMNH M 174860), *Homo* (CMNH HTH 0315), *Pongo* (USNM M 143596), and *Hylobates* (MCZ M 41455).

subarticular regions, *Homo* presents high rBV/TV across the sternal area, with peak values concentrated along the edges, particularly in the ventroinferior and dorsocranial directions (Figure 8). A comparable pattern is seen acromially, where a high rBV/TV is distributed throughout the entire region, with especially elevated concentrations at the dorsoventral edges.

The rBV/TV distribution in *Pongo* is notably more irregular compared to the other great apes (Figures 4–7). Clusters of elevated rBV/TV are observed around the lateral curvature and extend medially into the diaphysis, similar to *Pan*. However, in *Pongo*, these high values are typically concentrated more on the ventral and caudal aspects of the diaphysis rather than cranially (Figures 4–6). Additionally, similar to *Pan*, *Pongo* shows a region of high rBV/TV on the cranial aspect of the sternal diaphysis where the sternocleidomastoid muscle may have attached (Figure 4). In contrast to *Pan*, *Pongo* displays notably low rBV/TV in the dorsal aspect of the medial diaphysis, aligning more closely with *Homo* (Figure 7). The sternal subarticular region of *Pongo* shows elevated rBV/TV around its periphery, with lower rBV/TV in the center of the area (Figure 8). In the acromial region, rBV/TV is relatively high compared to other areas of the clavicle, but the distribution of these high values appears sporadic across the subarticular space.

Finally, *Hylobates*, the only lesser ape in the sample, displays a distinctive rBV/TV distribution across the clavicle (Figures 4–7). High rBV/TV is confined to the epiphyseal regions, with minimal trabecular bone present in the diaphysis. Sternally, *Hylobates* exhibits particularly elevated rBV/TV on the dorsoinferior aspect of the subarticular region (Figure 8). At the acromial end, a concentration of high rBV/TV is observed cranially, just medial to the articular surface, though these elevated values do not extend to the subarticular surface. The inferior aspect of the acromial region shows higher rBV/TV values compared to the cranial aspect, particularly where the coracoclavicular and acromioclavicular ligaments are expected to have attached.

3.2 | Trabecular thickness, separation, and number (Tb.Th, Tb.Sp, Tb.N)

Tb.Th, known to scale with body mass (Doube et al., 2011; Ryan & Shaw, 2013), is absolutely highest in *Gorilla* and lowest in *Hylobates* (Figure 3c; Table S4). With a slope of approximately 0.6 (Table 2; Figure 9), this relationship demonstrates negative allometry, indicating that while Tb.Th increases with bone length, the rate of increase is slower than proportional growth. However, when *Hylobates* is excluded, the relationship between Tb.Th and bone length becomes much weaker, with a near-flat slope of 0.002 among the great apes (Table 2; Figure 10). Among the great apes, *Pan* and *Pongo* exhibit slightly thinner trabeculae than *Gorilla*, while Tb.Th in *Homo* is comparable to *Gorilla* medially but resembles *Pan* and *Pongo* beyond 50% of the bone length (Figure 3c). *Hylobates*, by contrast, shows low Tb.Th in the sternal half of the clavicle, with a sharp increase around

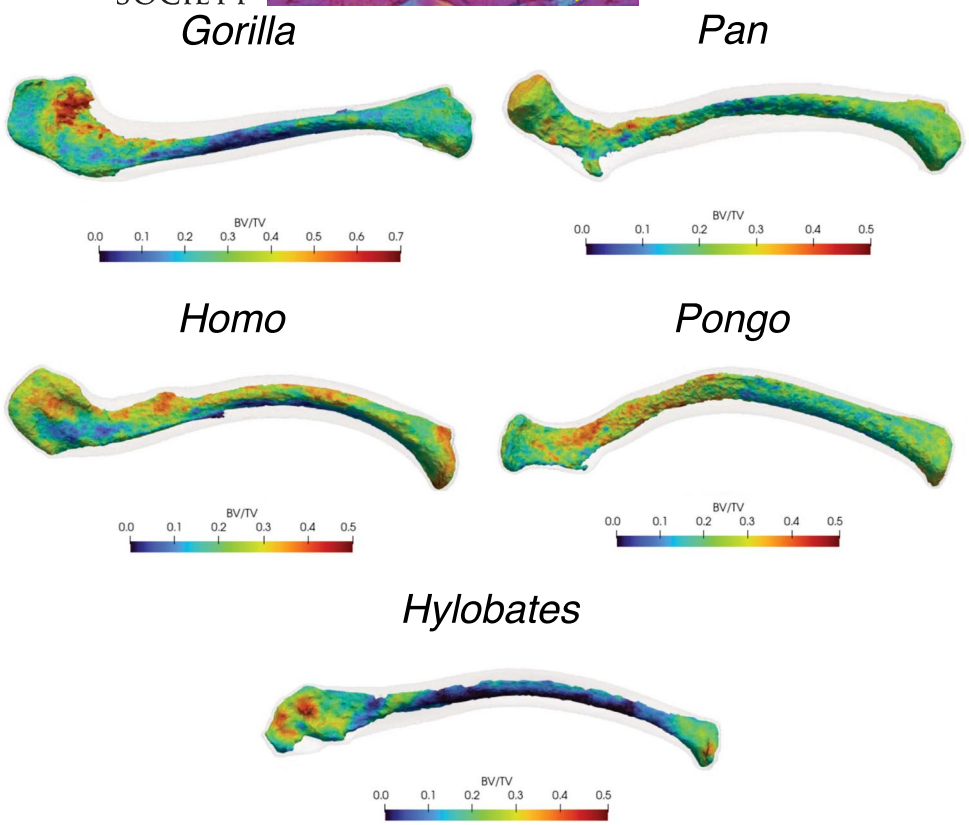

FIGURE 6 Intraspecific variation in BV/TV in the hominoid clavicle. Surface-level patterns of BV/TV in caudal view. The color map has been scaled based on the mean ± 3 standard deviations of BV/TV for each specimen, with warmer tones indicating higher BV/TV and cooler tones indicating lower BV/TV. Generic-level patterns are represented by the following specimens: *Gorilla* (AMNH M 167336), *Pan* (AMNH M 174860), *Homo* (CMNH HTH 0315), *Pongo* (USNM M 143596), and *Hylobates* (MCZ M 41455).

75% bone length, distinct from the more gradual increase observed in the great apes. Intraspecifically, Tb.Th scales with negative allometry in *Pan* (slope = 0.636; Table 2) and approaches isometry in *Homo* (slope = 0.973; Table 2), while no significant relationship is observed in the other ape taxa.

Tb.Sp exhibits distinct scaling patterns across apes. In all apes, Tb.Sp has a decreasing relationship with bone length, scaling with negative allometry (slope = −0.405; Table 2; Figure 9). However, among only the great apes, Tb.Sp shows an increasing relationship with bone length, also scaling with negative allometry (slope = 0.29; Table 2; Figure 10). No significant intraspecific scaling relationships are observed within any of the ape taxa. Looking at interspecific trends across the clavicle, *Hylobates* again stands out from the other apes, exhibiting a parabolic distribution with the highest trabecular separation in the diaphysis and lowest in the epiphyses (Figure 3d; Table S5). In contrast, all great apes show higher separation medially and lower separation laterally, with minor variations. *Homo* uniquely displays an increase in trabecular separation beyond 75% bone length, whereas the other apes exhibit decreasing separation in this region (Figure 3d). Among non-human great apes, *Gorilla* shows slightly more separation medially compared to *Pan* and *Pongo*, though these differences are not significant (Figure 3d; Table S5). Notably, *Pan* exhibits significantly lower separation than all other apes in the medial 20% of bone length (Table S5).

Tb.N exhibits relatively weak allometric relationships across the ape species. In all apes, there is a weak positive allometry (slope = 0.147; Table 2; Figure 9), while in the great apes, a weak negative allometry is observed (slope = − 0.274; Table 2; Figure 10). Generally, *Pan* and *Pongo* have higher Tb.N values compared to *Gorilla* and *Homo* (Figure 3e). *Homo* has significantly fewer trabeculae than *Pan* and *Pongo* in the acromial half of the clavicle (Table S6). Like rBV/TV, great apes exhibit a trend where Tb.N begins increasing around mid-diaphysis and peaks at approximately 75% bone length. *Hylobates* again differs by showing increased Tb.N only in the epiphyseal regions (Figure 3e). Despite these variations, all apes have more trabeculae per unit area in the epiphyses compared to the diaphyses, even in regions of the diaphysis with high rBV/TV. *Pan* uniquely exhibits an intraspecific allometric relationship between Tb.N and bone length (slope = − 0.622; Table 2), where larger individuals have fewer trabecular struts per unit area.

4 | DISCUSSION

This study aimed to explore the relationship between variation in trabecular bone distribution within the clavicle and the differing mechanical demands placed on the shoulder girdle across apes and modern humans. By investigating both subarticular regions and

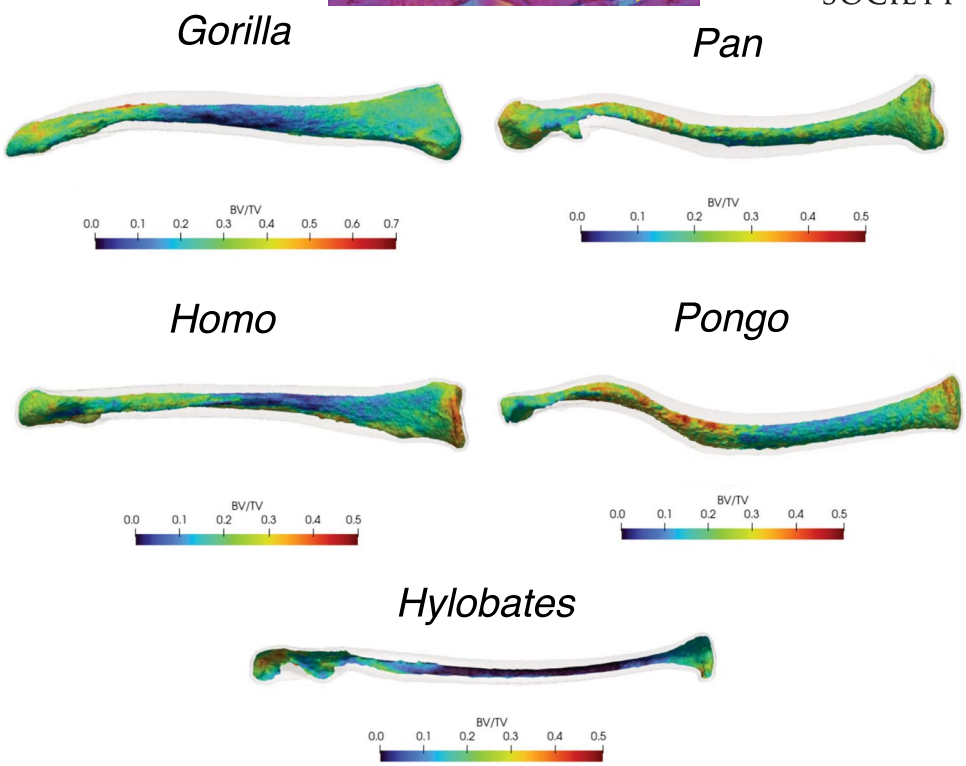

FIGURE 7 Intraspecific variation in BV/TV in the hominoid clavicle. Surface-level patterns of BV/TV in dorsal view. The color map has been scaled based on the mean ± 3 standard deviations of BV/TV for each specimen, with warmer tones indicating higher BV/TV and cooler tones indicating lower BV/TV. Generic-level patterns are represented by the following specimens: *Gorilla* (AMNH M 167336), *Pan* (AMNH M 174860), *Homo* (CMNH HTH 0315), *Pongo* (USNM M 143596), and *Hylobates* (MCZ M 41455).

muscle attachment sites, we seek to clarify the relationship between internal bone architecture and the habitual behaviors that define each species' unique locomotor and postural adaptations.

Among the apes, a clear distinction was found between the great apes (*Pan*, *Pongo*, *Gorilla*, and *Homo*) and the lesser apes (*Hylobates*) based on rBV/TV and related microstructural parameters such as trabecular number, separation, and thickness. *Hylobates*, in particular, displays a unique parabolic distribution of Tb.N and Tb.Sp, resulting in a low rBV/TV in the diaphysis that increases toward the epiphyses. In contrast, the great apes, while sharing general trends in trabecular structure, exhibit generic variations that reflect their distinct locomotor behaviors and functional demands. By examining these differences in trabecular structure, we can better understand the evolutionary adaptations that distinguish the apes.

4.1 | Differential patterns of BV/TV in Subarticular Regions

Our initial hypothesis predicted that suspensory taxa (*Pongo*, *Hylobates*) would exhibit decreased BV/TV in the subarticular regions of the clavicle due to tensile joint loading, whereas more terrestrial taxa (*Pan*, *Gorilla*) would show higher BV/TV due to compressive joint loading. This hypothesis was partially supported. Acromially, *Pan* and *Gorilla* exhibit higher BV/TV than *Pongo*, *Hylobates*, and *Homo*, aligning with expectations. However, these differences were not mirrored in the sternal subarticular region, where *Pan* displayed higher BV/TV than *Hylobates* and *Pongo*, but no significant differences were found between *Gorilla* and *Pongo*. This suggests that loading at the sternoclavicular joint may not conform strictly to the terrestrial–suspensory division initially proposed.

Additionally, the use of a whole-bone analysis to visualize rBV/TV throughout the clavicle revealed that the distribution of rBV/TV in the subarticular regions reflects the habitual range of motion at the sternoclavicular joint, rather than the orientation of the clavicle relative to the manubrium. This differs from findings in other skeletal elements, such as the first metacarpal in apes, where patterns of high BV/TV have been shown to correspond with regions experiencing the greatest joint reaction forces, driven by the distinct orientations of suspensory versus terrestrial hand postures (Dunmore et al., 2020; Tsegai et al., 2013). In *Homo*, high rBV/TV along the dorsoventral margins of the sternoclavicular subarticular area suggests an emphasis on dorsoventral rotation at the joint, likely facilitating scapular protraction and retraction to move the shoulder (Levangie & Norkin, 2001). This interpretation is supported by kinematic studies highlighting the importance of such scapular movements in high-velocity throwing (Kibler, 1998; Myers et al., 2005; Roach & Lieberman, 2014) and in various daily manipulative activities (Sheikhzadeh et al., 2008). Moreover, this distribution aligns with evidence of increased dorsoventral cortical reinforcement observed

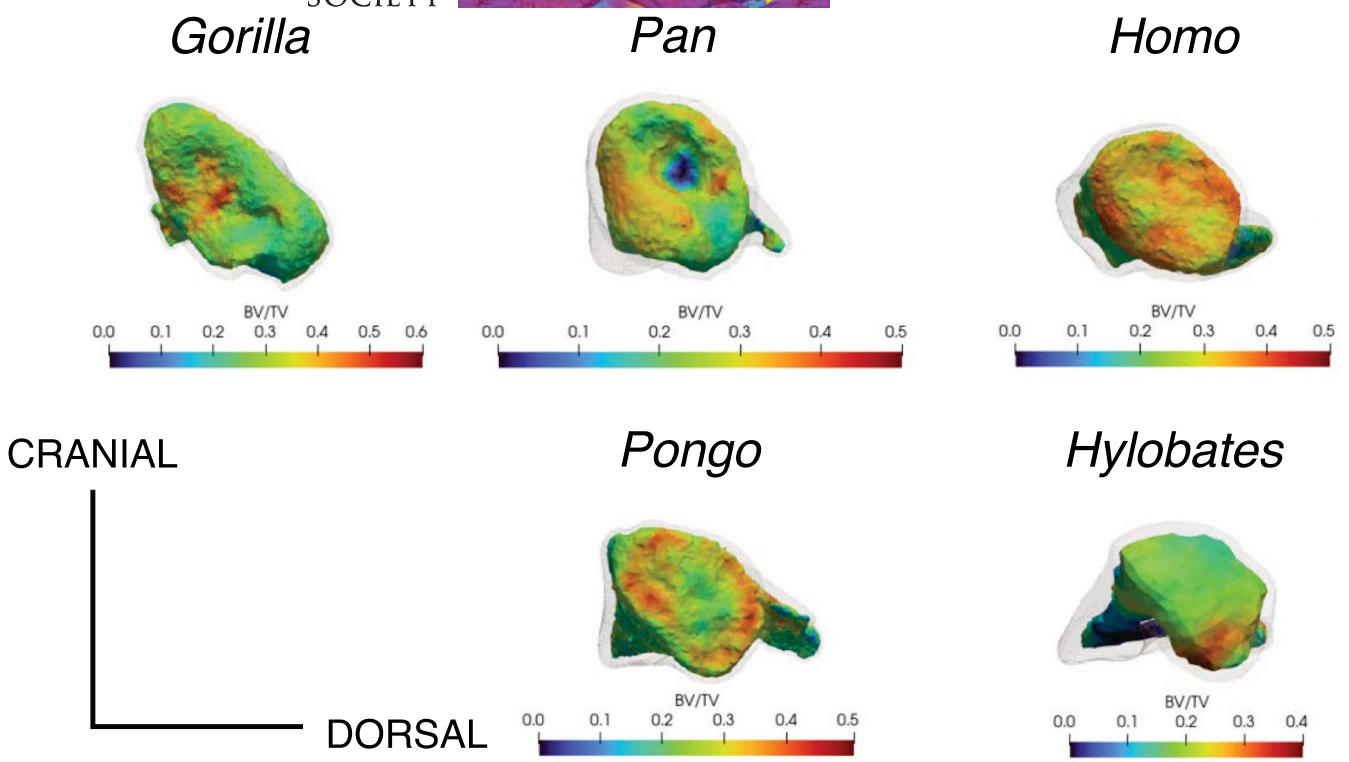

FIGURE 8 Intraspecific variation in trabecular bone volume fraction (BV/TV) within the sternal subarticular region of the hominoid clavicle. The figure displays surface-level patterns of BV/TV, with clavicles oriented such that the viewer is looking directly at the sternal subarticular surface. The orientation is as follows: Ventral to the left, dorsal to the right, cranial at the top, and caudal at the bottom. Warmer colors represent higher BV/TV, while cooler colors indicate lower BV/TV. Generic level patterns are represented by the following specimens: *Gorilla* (AMNH M 167336), *Pan* (AMNH M 174860), *Homo* (CMNH HTH 0315), *Pongo* (USNM M 143596), and *Hylobates* (MCZ M 41455).

in modern human clavicles, which suggests habitual dorsoventral bending loads (Farrell, 2024; Farrell and Alemseged, 2025). In *Pongo*, similarly high rBV/TV is present in the sternal epiphysis; however, trabecular bone is more distributed along the margins rather than concentrated centrally, likely reflecting a broader range of postures at the sternoclavicular joint compared to *Homo*. *Gorilla* shows a distinct pattern of high rBV/TV in the sternal subarticular region where increased rBV/TV is concentrated centrally and spreads variably cranioventrally among individuals. This likely reflects the stereotypic loading of the joint during knuckle walking and limited engagement in other behaviors that load the clavicle. However, this pattern does not fully align with expectations of protraction and retraction of the humeral head and scapula during knuckle walking (Hunt, 1991; Inouye, 1994). It is possible that the sternoclavicular joint in African apes, particularly *Gorilla*, exhibits reduced range of motion as an adaptation to stabilize the shoulder against shearing forces that could occur during knuckle walking due to the scapula's position and the thoracic shape (Inouye, 1994; Roberts, 1974). This supports the hypothesis that the inferiorly convex curvature of the medial clavicle in great apes, a feature largely absent in modern humans, helps maintain tension in the costoclavicular ligament, thereby restricting mobility at the sternoclavicular joint (Voisin, 2006). However, *Pan*, which exhibits the greatest degree of medial clavicular curvature (Farrell, 2024; Squyres & DeLeon, 2015; Voisin, 2006), shows a broader distribution of high rBV/TV across the sternal subarticular region, sharing similarities with both *Gorilla* and *Pongo*. This pattern may reflect *Pan*'s more arboreal lifestyle compared to *Gorilla* (Doran, 1997).

In the acromial subarticular region, rBV/TV displays a relatively consistent pattern across most apes, which is expected due to the limited range of motion at the acromioclavicular joint (Levangie & Norkin, 2001). *Homo*, however, stands out with increased rBV/TV along the dorsoventral margins, highlighting the clavicle's involvement in habitual and repetitive scapular movements, consistent with behaviors such as high-velocity throwing and daily manipulatory activities (Levangie & Norkin, 2001; Sheikhzadeh et al., 2008). Overall, the overlap in subarticular rBV/TV patterns among great apes parallels findings in the humeral head, where similar trabecular structures are observed across taxa (Kivell et al., 2018). Nevertheless, in the clavicle, these subarticular concentrations of high rBV/TV do not extend as deeply into the epiphysis in terrestrial apes as they do in their more suspensory relatives.

4.2 | Muscle and ligament attachment sites show higher BV/TV

In line with initial predictions, all great apes exhibit increased rBV/TV, to varying extents, in the dorsal region of the lateral curvature. This increase potentially reflects the recruitment of the

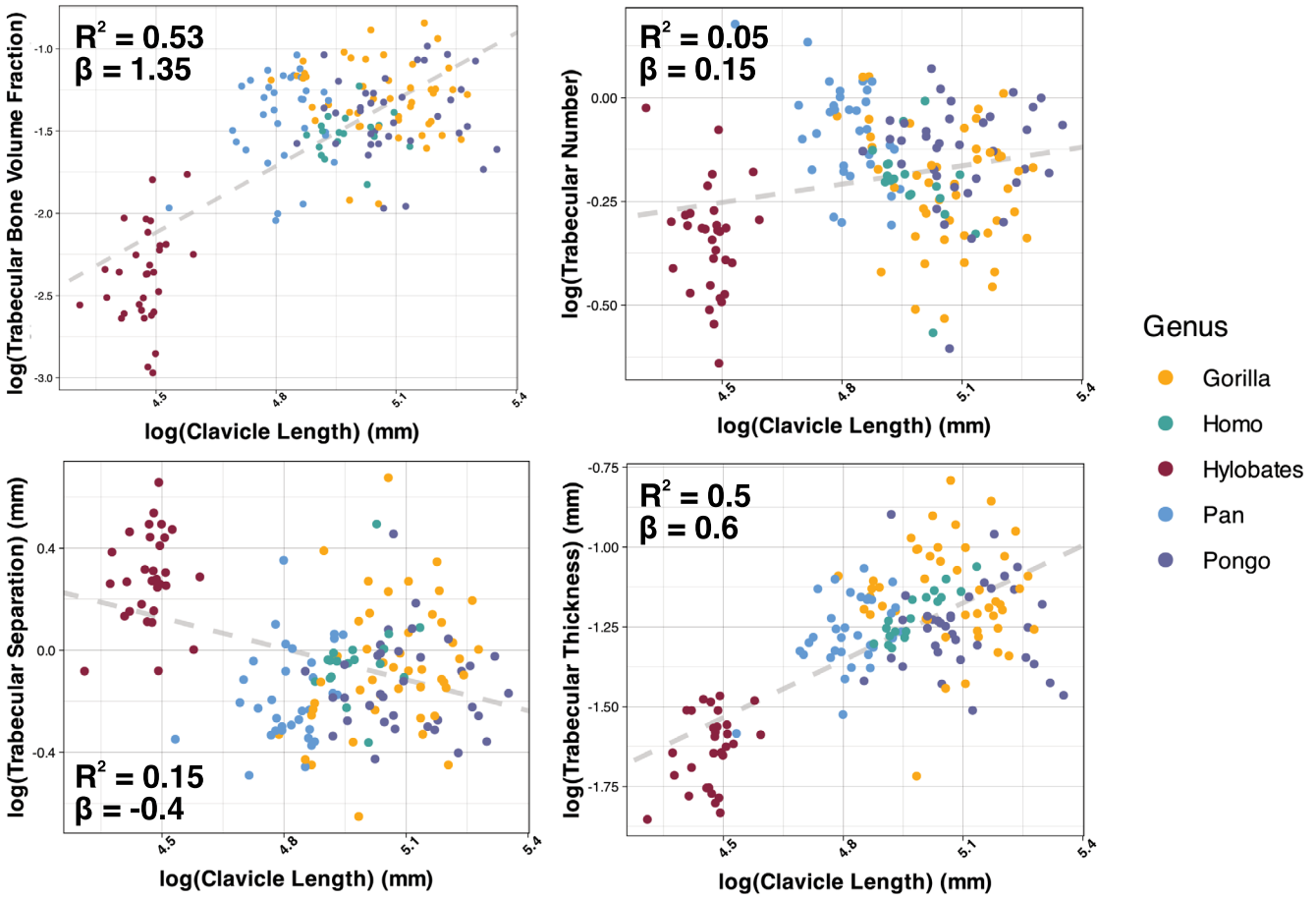

FIGURE 9 Allometric scaling trends of trabecular parameters relative to clavicular bone length, serving as a proxy for body mass across all apes. The x-axis shows log-transformed clavicular bone length, and the y-axis represents the log-transformed average value of each trabecular parameter across the entire clavicle for each individual. Data points are color-coded by genus. The R-squared value and slope for each linear regression is shown in the top left corner of each graph. For Tb.Th and Tb.Sp regressed against clavicular length, a slope (β) of 1 indicates isometry, with slopes above 1 indicating positive allometry and those below 1 indicating negative allometry. For BV/TV and Tb.N, a slope (β) of 0 indicates isometry, with positive values indicating positive allometry and negative values indicating negative allometry. Dashed lines indicate a statistically significant relationship.

cranial trapezius muscle during overhead arm swinging (Larson et al., 1991) and vertical climbing (Preuschoft et al., 2010). It may also be associated with the habitual use of the anterior deltoid muscle during behaviors such as arm elevation in climbing and arm retraction in knuckle walking (Larson & Stern, 1986; Larson & Stern, 1987). Although modern humans display overall lower BV/TV in this region compared to great apes, they still show a relative increase in rBV/TV in the lateral curvature compared to other parts of the clavicle. This pattern supports the findings of Wallace et al. (2017), who found that while elevated physical activity affects cortical and trabecular bone structure in the distal femoral epiphysis, it does not significantly alter entheseal surface topography. Similarly, studies by Zumwalt (2006), Rabey et al. (2015), and Djukic et al. (2015) failed to establish a direct link between entheseal morphology and physical activity. Notably, although muscle use signals were identified in the clavicle of great apes, the trabecular architecture of *Hylobates* clavicles does not reflect similar muscle recruitment patterns (Jungers & Stern, 1981; Stern et al., 1980), attachment sites (Diogo et al., 2012; Diogo & Wood, 2012), or muscle size (Michilsens et al., 2009) along the diaphysis. This lack of correspondence suggests that *Hylobates* trabecular structure does not align with the expected adaptations for brachiation. Overall, these results suggest that trabecular structure is a more reliable indicator of habitual physical activity than entheseal morphology, as it more accurately reflects changes in bone structure associated with mechanical loading.

All apes also show a concentration of increased rBV/TV on the inferior side of the acromial end near the attachment of the trapezoid ligament, which, along with the conoid ligament, connects the clavicle to the coronoid process of the scapula. This increase is particularly prominent in *Gorilla* and *Homo*, whereas in *Pan*, *Pongo*, and *Hylobates*, the elevated rBV/TV is present but more diffuse. The coracoclavicular ligaments, including the trapezoid ligament, are typically stretched or tightened during shoulder abduction, as the scapula rotates upward and externally, and the clavicle rotates posteriorly and retracts (Izadpanah et al., 2012; Lawrence et al., 2014;

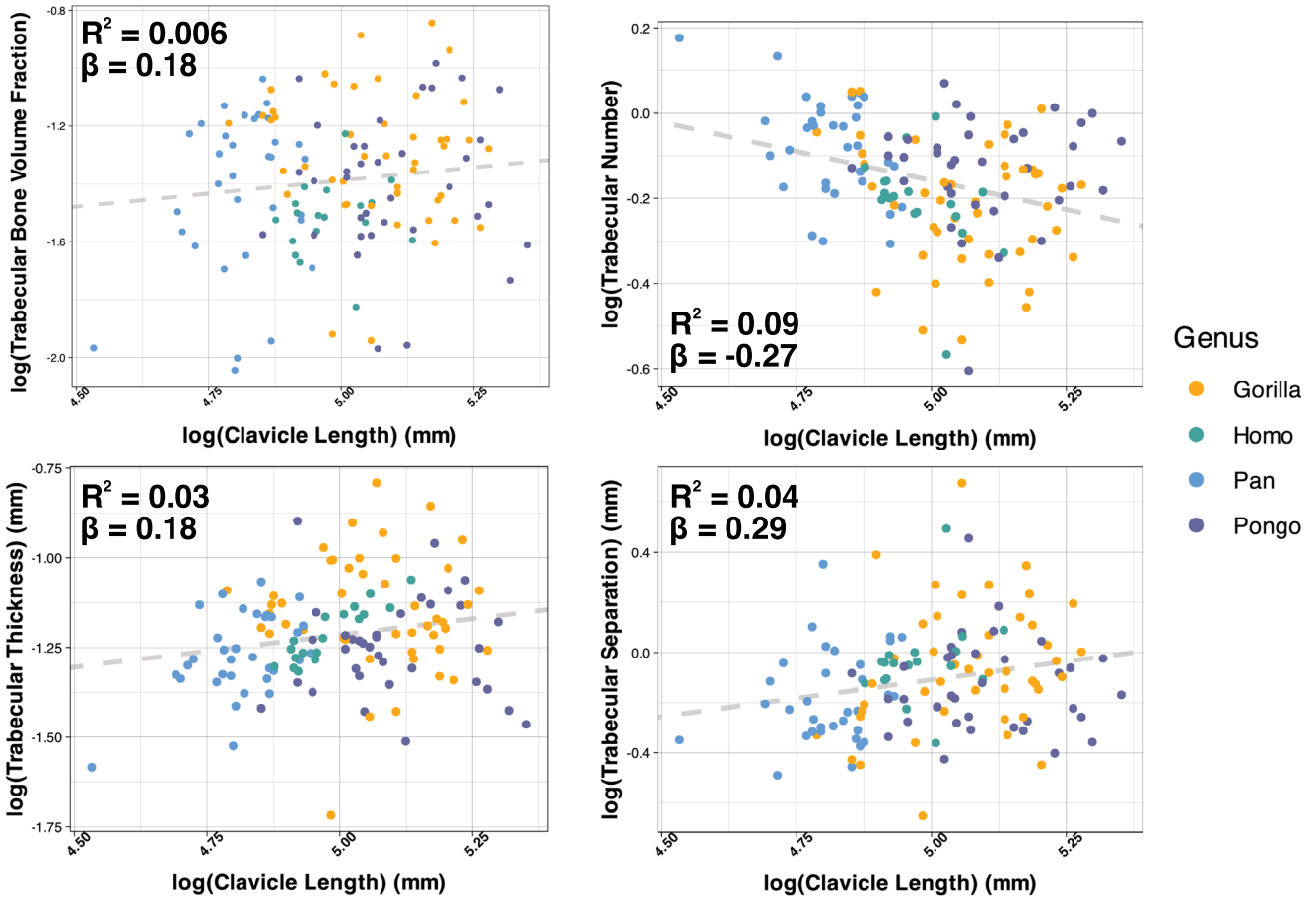

FIGURE 10 Allometric scaling trends of trabecular parameters relative to clavicular bone length, serving as a proxy for body mass across great apes. The *x*-axis shows log-transformed clavicular bone length, and the *y*-axis represents the log-transformed average value of each trabecular parameter across the entire clavicle for each individual. Data points are color-coded by genus. The R^2 value and slope for each linear regression is shown in the top left corner of each graph. For Tb.Th and Tb.Sp regressed against clavicular length, a slope (β) of 1 indicates isometry, with slopes above 1 indicating positive allometry and those below 1 indicating negative allometry. For BV/TV and Tb.N, a slope (β) of 0 indicates isometry, with positive values indicating positive allometry and negative values indicating negative allometry. Dashed lines indicate a statistically significant relationship.

Ludewig et al., 2009; Teece et al., 2008). Specifically, the trapezoid ligament acts to limit the internal rotation of the scapula in humans (Oki et al., 2012) and has been shown to experience more elastic strain than the acromioclavicular ligaments during humeral elevation and adduction, with peak strain occurring between 90–120 degrees of elevation and 80–100 degrees of adduction (Velasquez Garcia et al., 2023).

Bones subjected to tensile stress generally have a lower failure point than those subjected to compressive stress (Caler & Carter, 1989; Pattin et al., 1996). Consequently, greater trabecular bone volume fraction (BV/TV) or cortical thickness is required to prevent failure at ligament attachment sites (Doube et al., 2009). The observed patterns of increased rBV/TV in these regions likely reflect adaptation to high tensile forces, particularly in taxa with frequent arm use in specific ranges of motion. Supporting this interpretation, similar patterns of higher BV/TV associated with regions of ligament attachment have been observed in other skeletal elements, including the calcaneus (Biewener et al., 1996), the disto-radial flange of the first metacarpal (Dunmore et al., 2023), and the distal capitate (Bird et al., 2021).

Beyond variation in overall trabecular bone volume fraction, consistent patterns in trabecular number and thickness across great apes suggest a shared mechanism driving trabecular bone adaptation. In regions of muscle attachment, increased relative trabecular bone volume fraction (rBV/TV) results from a combination of greater trabecular number and thickness, along with reduced trabecular separation (Schwartz et al., 2024). This aligns with findings of thicker trabecular bone in the distal femur of exercised animals compared to controls (Wallace et al., 2017) and reduced trabecular thickness in tenotomized calcanei (Biewener et al., 1996). The increased trabecular thickness in these regions likely reinforces the cortical bone, enhancing structural support and stability. Conversely, in subarticular regions, the elevated rBV/TV is mainly due to a higher trabecular number and decreased separation (Schwartz et al., 2024). This pattern suggests that increased trabecular number in these regions helps better distribute forces across a larger area, optimizing the

bone's ability to manage the stresses associated with substrate reaction forces at the joint. This contrast highlights different responses to the compressive forces within joints versus the tensile stresses from muscle contractions.

Collectively, these findings underscore that trabecular bone structure serves as a reliable indicator of mechanical loading, particularly in regions subjected to significant tensile stress.

4.3 | Unique trabecular trend in *Homo sapiens*

The trabecular bone structure of the modern human clavicle presents distinct characteristics that set it apart from other great apes. Notably, modern humans exhibit increased BV/TV in the ventral portion of the medial diaphysis relative to the other apes, where the clavicular pectoralis major muscle originates. This muscle is essential for arm flexion up to 90°, adduction, and medial rotation (Barberini, 2014), playing a significant role in object manipulation. Although modern humans exhibit lower BV/TV in the lateral half of the clavicle compared to non-human great apes, the elevated BV/TV in the medial diaphysis means that the overall bone volume fraction in the medial clavicle remains relatively consistent across great apes. While this initially appears in contrast with previous research suggesting recent gracilization of the modern human trabecular structure (Chirchir et al., 2015; Ryan & Shaw, 2015), the increased BV/TV in the medial diaphysis supports the hypothesis that a sedentary lifestyle in modern humans contributes to a lower BV/TV in other regions (Chirchir et al., 2015; Ryan & Shaw, 2015), as the pectoralis major is likely engaged more frequently and intensely in modern humans than in extant apes (Larson & Stern, 1986; Larson & Stern, 1987; Lulic-Kuryllo et al., 2021). Further, when BV/TV is standardized across taxa, modern humans show comparable rBV/TV values throughout the clavicle relative to great apes. In combination with observations of reduced BV/TV in the humerus (Kivell et al., 2018) and carpals (Bird et al., 2021; Bird et al., 2022) of modern humans, this pattern may suggest a similar proximodistal gradient of BV/TV reduction in the upper limb as seen in the lower limb (Saers et al., 2016).

Even though modern humans show lower mean values of BV/TV and rBV/TV compared to great apes through the lateral diaphysis, the whole-bone visualization of trabecular trends reveals that *Homo* exhibits increased rBV/TV around the lateral curvature in regions similar to those seen in non-human great apes. Notably, modern humans display a distinctive pattern with high rBV/TV concentrated more ventrally on the clavicle's lateral curvature, in contrast to the more cranial orientation observed in *Pan* and *Gorilla*. This variation is likely related to the more ventral attachment of the anterior deltoid muscle in modern humans (Diogo & Wood, 2012; Larson, 2007; Swindler & Wood, 1973), which is involved in flexing and internally rotating the arm during object manipulation.

Interestingly, the increased rBV/TV in the region of the cranial trapezius in modern humans was unexpected, given that in non-human apes this pattern is potentially linked to the muscle's involvement in overhead arm swinging and climbing. In humans, however, this elevated rBV/TV appears to be more related to postural stabilization. In modern humans, the cranial trapezius passively stabilizes the pectoral girdle against the downward load imposed by the pendular upper limb and transmits forces to the sternoclavicular joint through its attachment on the lateral clavicle (Gaffney et al., 2014; Gonçalves et al., 2017; Johnson et al., 1994), rather than chiefly contributing to head stabilization or movement (Keshner et al., 1989). This increased loading relative to non-human apes likely contributes to the elevated rBV/TV observed in the dorsal region of the lateral clavicle. The increase in rBV/TV may be due to the combination of near-continuous background activation required to support the shoulder girdle in bipedal posture, along with habitual activation for upper limb movements and head flexion. It is also important to consider the composition of the representative modern human sample, which predominantly represents poor post-industrial individuals, likely factory workers or laborers. This group may have experienced higher trapezius activation due to increased physical stress and repetitive, less-rested movements (Jensen et al., 1993).

In sum, examining trabecular bone distribution in both the diaphysis and subarticular epiphysis of the clavicle reveals insights into the locomotor behaviors and functional adaptations of apes. For *Pongo*, the trabecular morphology suggests extensive mobility at the sternoclavicular joint, supporting diverse arboreal activities such as arm flexion facilitated by the anterior deltoid and head stabilization provided by the cranial trapezius. In *Gorilla*, the trabecular pattern indicates significant forelimb retraction during knuckle walking, driven by the anterior deltoid. *Pan* shows an intermediate trabecular structure, reflecting a blend of arboreal and terrestrial activities. In *Homo*, the trabecular distribution suggests a primary use of the forelimb in the dorsoventral plane, with the clavicular pectoralis major and anterior deltoid playing key roles in arm flexion, adduction, and medial rotation during object manipulation.

5 | CONCLUSION

Ultimately, this study demonstrates that the trabecular architecture of the clavicle across different ape taxa provides critical insights into their distinct locomotor behaviors and functional adaptations. As the first analysis to directly investigate trabecular bone distribution patterns in relation to muscle insertion within a comparative framework, it reveals key patterns such as generally higher trabecular number in the epiphyses and increased trabecular thickness underlying muscle entheses. Additionally, the study shows that in extant apes, increased trabecular bone volume fraction is concentrated in areas associated with the attachment of muscles frequently engaged during locomotion, supporting hypotheses that bone deposition can be more responsive to tensile forces than compressive ones (Bird et al., 2021; Bird et al., 2022; Doube et al., 2009; Pattin et al., 1996). This pattern not only demonstrates how muscle activity influences bone structure in living apes, but also offers a framework for interpreting muscle use in fossil hominins. For instance, elevated BV/TV

in the region associated with the pectoralis major may signify a shift toward greater reliance on the arms for manipulation and reduced use of the arboreal environment. Similarly, a ventrally located concentration of high BV/TV at the lateral end may indicate a shift in the anterior deltoid attachment site, highlighting adaptations in shoulder function and upper limb use. By highlighting differences in trabecular architecture across hominoid taxa, this study advances our understanding of primate shoulder evolution and lays the groundwork for future research into the adaptive significance of bone microstructure in relation to locomotor behavior and muscle function.

AUTHOR CONTRIBUTIONS

HF and ZA conceived and designed the study. HF and RS collected the data. HF analyzed the results, with RS, ZT, and ZA assisting with the interpretations. HF drafted, and ZT and ZA edited the manuscript. HF, RS, ZT, and ZA revised the manuscript.

ACKNOWLEDGEMENTS

For access to the extant ape skeletal material, we thank Adam Ferguson (FMNH), Lawrence Heaney (FMNH), Bruce Patterson (FMNH), Anderson Fiejó (FMNH), Marisa Surovy (AMNH), Neil Duncan (AMNH), Darrin Lunde (USNM), Megan Viera (USNM), Mark Omura (Harvard MCZ), Roman Wittig (TCP), Catherine Crockford (TCP), Tracy Kivell (MPI), and Philipp Gunz (MPI). We would also like to thank the micro-CT technicians and facility managers Zhe-Xi Luo (Chicago), April Neander (Chicago), Greg Lin (Harvard CNS), James Reynolds (Harvard CNS), and Heiko Temming (MPI). Financial support for data acquisition and analysis was provided by the Leakey Foundation, National Science Foundation (grant number 2317012), University of Chicago Hinds Fund, and University of Chicago support of the Alemseged Lab Paleoanthropology Program. Special thanks to Margaret and Will Hearst for their generous support of this research. We also thank Callum Ross, Zhe-Xi Luo, Weldeyared Reda, Laura Hunter, Madeline Kelly, Alec Wilken, and Emily Hillan for their valuable discussions and insights on this work. Finally, we extend our gratitude to the two anonymous reviewers for their constructive feedback, which greatly improved this manuscript.

DATA AVAILABILITY STATEMENT

The data that support the findings of this study, along with the code used for analyses, are available from the corresponding author upon reasonable request.

ORCID

Hannah N. Farrell https://orcid.org/0009-0004-7692-088X
Zewdi J. Tsegai https://orcid.org/0000-0001-9041-4829

REFERENCES

Ahrens, J., Geveci, B. & Law, C. (2005) 36 – ParaView: an end-user tool for large-data visualization. In: Hansen, C.D. & Johnson, C.R. (Eds.) *Visualization Handbook*. Butterworth-Heinemann, pp. 717–731. Available from: https://doi.org/10.1016/B978-012387582-2/50038-1. isbn:9780123875822. Available from: https://www.sciencedirect.com/science/article/pii/B9780123875822500381

Almécija, S., Hammond, A.S., Thompson, N.E., Pugh, K.D., Moyà-Solà, S. & Alba, D.M. (2021) Fossil apes and human evolution. *Science*, 372, Article eabb4363. Available from: https://doi.org/10.1126/science.abb4363

Arias-Martorell, J., Potau, J.M., Bello-Hellegouarch, G. & Pérez-Pérez, A. (2015) Like father, like son: assessment of the morphological affinities of a.L. 288–1 (a. afarensis), Sts 7 (a. africanus) and Omo 119–73–2718 (Australopithecus sp.) through a three-dimensional shape analysis of the shoulder joint. *PLoS One*, 10, e0117408. Available from: https://doi.org/10.1371/journal.pone.0117408

Barak, M.M., Lieberman, D.E. & Hublin, J.-J. (2011) A Wolff in sheep's clothing: trabecular bone adaptation in response to changes in joint loading orientation. *Bone*, 49, 1141–1151. Available from: https://doi.org/10.1016/j.bone.2011.08.020

Barak, M.M., Lieberman, D.E., Raichlen, D., Pontzer, H., Warrener, A.G. & Hublin, J.-J. (2013) Trabecular evidence for a human-like gait in Australopithecus africanus. *PLoS One*, 8, e77687. Available from: https://doi.org/10.1371/journal.pone.0077687

Barak, M.M., Weiner, S. & Shahar, R. (2008) Importance of the integrity of trabecular bone to the relationship between load and deformation of rat femora: an optical metrology study. *Journal of Materials Chemistry*, 18, 3855–3864.

Barberini, F. (2014) The clavicular part of the pectoralis major: a true entity of the upper limb on anatomical, phylogenetic, ontogenetic, functional and clinical bases: case report and review of the literature. *IJAE: Italian Journal of Anatomy and Embryology*, 119, 49–59. Available from: https://doi.org/10.1400/227237

Barros, A.P. (2014) Ontogeny, phylogeny and functional morphology of the hominoid shoulder girdle (Doctoral). Doctoral thesis, UCL (University College London). UCL (University College London).

Benjamin, M., Kaiser, E. & Milz, S. (2008) Structure-function relationships in tendons: a review. *Journal of Anatomy*, 212, 211–228. Available from: https://doi.org/10.1111/j.1469-7580.2008.00864.x

Benjamin, M. & McGonagle, D. (2009) Entheses: tendon and ligament attachment sites. *Scandinavian Journal of Medicine & Science in Sports*, 19, 520–527. Available from: https://doi.org/10.1111/j.1600-0838.2009.00906.x

Benjamin, M. & Ralphs, J.R. (1997) Tendons and ligaments--an overview. *Histology and Histopathology*, 12, 1135–1144.

Biewener, A.A., Fazzalari, N.L., Konieczynski, D.D. & Baudinette, R.V. (1996) Adaptive changes in trabecular architecture in relation to functional strain patterns and disuse. *Bone*, 19, 1–8. Available from: https://doi.org/10.1016/8756-3282(96)00116-0

Bird, E.E., Kivell, T.L. & Skinner, M.M. (2021) Cortical and trabecular bone structure of the hominoid capitate. *Journal of Anatomy*, 239, 351–373. Available from: https://doi.org/10.1111/joa.13437

Bird, E.E., Kivell, T.L. & Skinner, M.M. (2022) Patterns of internal bone structure and functional adaptation in the hominoid scaphoid, lunate, and triquetrum. *American Journal of Biological Anthropology*, 177, 266–285. Available from: https://doi.org/10.1002/ajpa.24449

Caler, W.E. & Carter, D.R. (1989) Bone creep-fatigue damage accumulation. *Journal of Biomechanics*, 22, 625–635. Available from: https://doi.org/10.1016/0021-9290(89)90013-4

Carter, D., Orr, T. & Fyhrie, D.P. (1989) Relationships between loading history and femoral cancellous bone architecture. *Journal of Biomechanics*, 22, 231–244.

Chirchir, H., Kivell, T.L., Ruff, C.B., Hublin, J.-J., Carlson, K.J., Zipfel, B. et al. (2015) Recent origin of low trabecular bone density in modern humans. *Proceedings of the National Academy of Sciences*, 112, 366–371. Available from: https://doi.org/10.1073/pnas.1411696112

Chirchir, H., Zeininger, A., Nakatsukasa, M., Ketcham, R.A. & Richmond, B.G. (2017) Does trabecular bone structure within the metacarpal heads of primates vary with hand posture? *Comptes Rendus Palevol*, 16, 533–544. Available from: https://doi.org/10.1016/j.crpv.2016.10.002

Corrigan, G.E. (1960) The neonatal clavicle. *Neo*, 2, 79–92. Available from: https://doi.org/10.1159/000239790

Cotter, M.M., Simpson, S.W., Latimer, B.M. & Hernandez, C.J. (2009) Trabecular microarchitecture of hominoid thoracic vertebrae. *The Anatomical Record: Advances in Integrative Anatomy and Evolutionary Biology: Advances in Integrative Anatomy and Evolutionary Biology*, 292, 1098–1106.

Cowgill, L.W. (2007) Humeral torsion revisited: a functional and ontogenetic model for populational variation. *American Journal of Physical Anthropology*, 134, 472–480. Available from: https://doi.org/10.1002/ajpa.20689

Crompton, R.H., Vereecke, E.E. & Thorpe, S.K.S. (2008) Locomotion and posture from the common hominoid ancestor to fully modern hominins, with special reference to the last common panin/hominin ancestor. *Journal of Anatomy*, 212, 501–543. Available from: https://doi.org/10.1111/j.1469-7580.2008.00870.x

Currey, J. (2002) *Bones: structure and mechanics*. Princeton: Princeton University Press. Available from: https://doi-org.proxy.uchicago.edu/10.1515/9781400849505

Currey, J.D., Dean, M.N. & Shahar, R. (2017) Revisiting the links between bone remodelling and osteocytes: insights from across phyla. *Biological Reviews*, 92, 1702–1719. Available from: https://doi.org/10.1111/brv.12302

DeSilva, J.M. & Devlin, M.J. (2012) A comparative study of the trabecular bony architecture of the talus in humans, non-human primates, and Australopithecus. *Journal of Human Evolution*, 63, 536–551. Available from: https://doi.org/10.1016/j.jhevol.2012.06.006

Diogo, R., Potau, J.M., Pastor, J.F., dePaz, F.J., Ferrero, E.M., Bello, G. et al. (2012) *Photographic and descriptive musculoskeletal atlas of gibbons and siamangs (Hylobates): with notes on the attachments, variations, innervation, synonymy and weight of the muscles*, 1st edition. CRC Press. https://doi-org.proxy.uchicago.edu/10.1201/b11936

Diogo, R. & Wood, B. (2011) Soft-tissue anatomy of the primates: phylogenetic analyses based on the muscles of the head, neck, pectoral region and upper limb, with notes on the evolution of these muscles. *Journal of Anatomy*, 219, 273–359. Available from: https://doi.org/10.1111/j.1469-7580.2011.01403.x

Diogo, R. & Wood, B.A. (2012) *Comparative anatomy and phylogeny of primate muscles and human evolution*, 1st edition. CRC Press. Available from: https://doi-org.proxy.uchicago.edu/10.1201/b11605

Djukic, K., Milovanovic, P., Hahn, M., Busse, B., Amling, M. & Djuric, M. (2015) Bone microarchitecture at muscle attachment sites: the relationship between macroscopic scores of entheses and their cortical and trabecular microstructural design. *American Journal of Physical Anthropology*, 157, 81–93. Available from: https://doi.org/10.1002/ajpa.22691

Doran, D.M. (1997) Ontogeny of locomotion in mountain gorillas and chimpanzees. *Journal of Human Evolution*, 32, 323–344. Available from: https://doi.org/10.1006/jhev.1996.0095

Doube, M., Conroy, A.W., Christiansen, P., Hutchinson, J.R. & Shefelbine, S. (2009) Three-dimensional geometric analysis of felid limb bone allometry. *PLoS One*, 4, e4742. Available from: https://doi.org/10.1371/journal.pone.0004742

Doube, M., Kłosowski, M.M., Wiktorowicz-Conroy, A.M., Hutchinson, J.R. & Shefelbine, S.J. (2011) Trabecular bone scales allometrically in mammals and birds. *Proceedings of the Royal Society B: Biological Sciences*, 278, 3067–3073. Available from: https://doi.org/10.1098/rspb.2011.0069

Drapeau, M.S.M. (2004) Functional anatomy of the olecranon process in hominoids and plio-pleistocene hominins. *American Journal of Physical Anthropology*, 124, 297–314. Available from: https://doi.org/10.1002/ajpa.10359

Dunmore, C.J., Bachmann, S., Synek, A., Pahr, D.H., Skinner, M.M. & Kivell, T.L. (2023) The deep trabecular structure of first metacarpals in extant hominids. *American Journal of Biological Anthropology*, 183, 24695. Available from: https://doi.org/10.1002/ajpa.24695

Dunmore, C.J., Bardo, A., Skinner, M.M. & Kivell, T.L. (2020) Trabecular variation in the first metacarpal and manipulation in hominids. *American Journal of Physical Anthropology*, 171, 219–241. Available from: https://doi.org/10.1002/ajpa.23974

Dunmore, C.J., Wollny, G. & Skinner, M.M. (2018) MIA-clustering: a novel method for segmentation of paleontological material. *PeerJ*, 6, e4374. Available from: https://doi.org/10.7717/peerj.4374

Ehrlich, P.J. & Lanyon, L.E. (2002) Mechanical strain and bone cell function: a review. *Osteoporosis International*, 13, 688–700. Available from: https://doi.org/10.1007/s001980200095

Eriksen, E.F. (1986) Normal and pathological remodeling of human trabecular bone: three dimensional reconstruction of the remodeling sequence in normals and in metabolic bone disease. *Endocrine Reviews*, 7, 379–408.

Eriksen, E.F. (2010) Cellular mechanisms of bone remodeling. *Reviews in Endocrine and Metabolic Disorders*, 11, 219–227.

Farrell, H.N. (2024) Identifying Locomotor Adaptations in the Hominoid Clavicle and the Implications for Interpreting Hominin Behavior (Ph.D.). The University of Chicago, United States, Illinois.

Farrell, H.N. & Alemseged, Z. (2025) Locomotor adaptation in the hominoid clavicle through ontogeny. *Journal of Human Evolution*, 201, 103652. Available from: https://doi.org/10.1016/j.jhevol.2025.103652

Gaffney, B.M., Maluf, K.S., Curran-Everett, D. & Davidson, B.S. (2014) Associations between cervical and scapular posture and the spatial distribution of trapezius muscle activity. *Journal of Electromyography and Kinesiology*, 24, 542–549. Available from: https://doi.org/10.1016/j.jelekin.2014.04.008

Georgiou, L., Kivell, T.L., Pahr, D.H., Buck, L.T. & Skinner, M.M. (2019) Trabecular architecture of the great ape and human femoral head. *Journal of Anatomy*, 234, 679–693. Available from: https://doi.org/10.1111/joa.12957

Gonçalves, J.S., Shinohara Moriguchi, C., Takekawa, K.S., Coury, H.J.C.G. & Sato, T.d.O. (2017) The effects of forearm support and shoulder posture on upper trapezius and anterior deltoid activity. *Journal of Physical Therapy Science*, 29, 793–798. Available from: https://doi.org/10.1589/jpts.29.793

Gordon, J.E. (1978) Structures: or why things don't fall down. *Da Capo*. ISBN-10: 0-306-81283-5; ISBN-13: 978-0-306-81283-5.

Green, D. (2013) Ontogeny of the hominoid scapula: the influence of locomotion on morphology. *American Journal of Physical Anthropology*, 152, 239–260. Available from: https://doi.org/10.1002/ajpa.22353

Green, D. & Alemseged, Z. (2012) Australopithecus afarensis scapular ontogeny, function, and the role of climbing in human evolution. *Science*, 338, 514–517. Available from: https://doi.org/10.1126/science.1227123

Gross, T., Kivell, T., Skinner, M., Nguyen, N. & Pahr, D. (2014) A CT-image-based framework for the holistic analysis of cortical and trabecular bone morphology. *Palaeontologia Electronica*, 17, 33. Available from: https://doi.org/10.26879/438

Harrington, M.A., Keller, T.S., Seiler, J.G., Weikert, D.R., Moeljanto, E. & Schwartz, H.S. (1993) Geometric properties and the predicted mechanical behavior of adult human clavicles. *Journal of Biomechanics*, 26, 417–426. Available from: https://doi.org/10.1016/0021-9290(93)90005-Y

Hildebrand, T. & Rüegsegger, P. (1997) A new method for the model-independent assessment of thickness in three-dimensional images. *Journal of Microscopy*, 185, 67–75. Available from: https://doi.org/10.1046/j.1365-2818.1997.1340694.x

Huiskes, R., Ruimerman, R., van Lenthe, G.H. & Janssen, J.D. (2000) Effects of mechanical forces on maintenance and adaptation of form in trabecular bone. *Nature*, 405, 704–706. Available from: https://doi.org/10.1038/35015116

Hunt, K.D. (1991) Mechanical implications of chimpanzee positional behavior. *American Journal of Physical Anthropology*, 86, 521–536. Available from: https://doi.org/10.1002/ajpa.1330860408

Inouye, S.E. (1994) The ontogeny of knuckle-walking behavior and associated morphology in the African apes. (Volumes I and II) (Ph.D.). Northwestern University, United States – Illinois.

Izadpanah, K., Weitzel, E., Honal, M., Winterer, J., Vicari, M., Maier, D. et al. (2012) In vivo analysis of coracoclavicular ligament kinematics during shoulder abduction. *The American Journal of Sports Medicine*, 40, 185–192. Available from: https://doi.org/10.1177/0363546511423015

Jacobs, C.R. (2000) The mechanobiology of cancellous bone structural adaptation. *Journal of Rehabilitation Research and Development*, 37, 209–216.

Jensen, C., Nilsen, K., Hansen, K. & Westgaard, R.H. (1993) Trapezius muscle load as a risk indicator for occupational shoulder-neck complaints. *International Archives of Occupational and Environmental Heath*, 64, 415–423. Available from: https://doi.org/10.1007/BF00517947

Johnson, G., Bogduk, N., Nowitzke, A. & House, D. (1994) Anatomy and actions of the trapezius muscle. *Clinical Biomechanics*, 9, 44–50. Available from: https://doi.org/10.1016/0268-0033(94)90057-4

Judex, S., Garman, R., Squire, M., Donahue, L.-R. & Rubin, C. (2004) Genetically based influences on the site-specific regulation of trabecular and cortical bone morphology. *Journal of Bone and Mineral Research*, 19, 600–606.

Jungers, W.L. & Stern, J.T. (1981) Preliminary electromyographical analysis of brachiation in gibbon and spider monkey. *International Journal of Primatology*, 2, 19–33. Available from: https://doi.org/10.1007/BF02692297

Kagaya, M., Ogihara, N. & Nakatsukasa, M. (2010) Is the clavicle of apes long? An investigation of clavicular length in relation to body mass and upper thoracic width. *International Journal of Primatology*, 31, 209–217. Available from: https://doi.org/10.1007/s10764-010-9402-x

Keaveny, T.M., Morgan, E.F., Niebur, G.L. & Yeh, O.C. (2001) Biomechanics of trabecular bone. *Annual Review of Biomedical Engineering*, 3, 307–333.

Keshner, E.A., Campbell, D., Katz, R.T. & Peterson, B.W. (1989) Neck muscle activation patterns in humans during isometric head stabilization. *Experimental Brain Research*, 75, 335–344. Available from: https://doi.org/10.1007/BF00247939

Kibler, W.B. (1998) The role of the scapula in athletic shoulder function. *The American Journal of Sports Medicine*, 26, 325–337. Available from: https://doi.org/10.1177/03635465980260022801

Kivell, T.L. (2016) A review of trabecular bone functional adaptation: what have we learned from trabecular analyses in extant hominoids and what can we apply to fossils? *Journal of Anatomy*, 228, 569–594. Available from: https://doi.org/10.1111/joa.12446

Kivell, T.L., Davenport, R., Hublin, J.-J., Thackeray, J.F. & Skinner, M.M. (2018) Trabecular architecture and joint loading of the proximal humerus in extant hominoids, Ateles, and Australopithecus africanus. *American Journal of Physical Anthropology*, 167, 348–365. Available from: https://doi.org/10.1002/ajpa.23635

Larson, S.G. (2007) Evolutionary transformation of the hominin shoulder. *Evolutionary Anthropology: Issues, News, and Reviews*, 16, 172–187. Available from: https://doi.org/10.1002/evan.20149

Larson, S.G. (2013) Shoulder morphology in early hominin evolution. In: Reed, K.E., Fleagle, J.G. & Leakey, R.E. (Eds.) *The paleobiology of Australopithecus, vertebrate paleobiology and paleoanthropology*. Dordrecht: Springer Netherlands, pp. 247–261. Available from: https://doi.org/10.1007/978-94-007-5919-0_17

Larson, S.G. & Stern, J.T. (1986) EMG of scapulohumeral muscles in the chimpanzee during reaching and "arboreal" locomotion. *The American Journal of Anatomy*, 176, 171–190. Available from: https://doi.org/10.1002/aja.1001760207

Larson, S.G. & Stern, J.T. (1987) EMG of chimpanzee shoulder muscles during knuckle-walking: problems of terrestrial locomotion in a suspensory adapted primate. *Journal of Zoology*, 212, 629–655. Available from: https://doi.org/10.1111/j.1469-7998.1987.tb05961.x

Larson, S.G., Stern, J.T. & Jungers, W.L. (1991) EMG of serratus anterior and trapezius in the chimpanzee: scapular rotators revisited. *American Journal of Physical Anthropology*, 85, 71–84. Available from: https://doi.org/10.1002/ajpa.1330850109

Laudicina, N.M. & Cartmill, M. (2023) Clavicle length and shoulder breadth in hominoid evolution. *The Anatomical Record*, 306, 2090–2101. Available from: https://doi.org/10.1002/ar.25144

Lawrence, R.L., Braman, J.P., LaPrade, R.F. & Ludewig, P.M. (2014) Comparison of 3-dimensional shoulder complex kinematics in individuals with and without shoulder pain, part 1: sternoclavicular, acromioclavicular, and scapulothoracic joints. *Journal of Orthopaedic & Sports Physical Therapy*, 44, 636–645. Available from: https://doi.org/10.2519/jospt.2014.5339

Levangie, P.K. & Norkin, C.C. (2001) *Joint structure and function: a comprehensive analysis*, 3rd. edition. Philadelphia: F. A. Davis.

Lieberman, D.E., Devlin, M.J. & Pearson, O.M. (2001) Articular area responses to mechanical loading: effects of exercise, age, and skeletal location. *American Journal of Physical Anthropology*, 116, 266–277. Available from: https://doi.org/10.1002/ajpa.1123

Ljunggren, A.E. (1979) Clavicular Function. *Acta Orthopaedica Scandinavica*, 50, 261–268. Available from: https://doi.org/10.3109/17453677908989766

Lovejoy, C.O., McCollum, M.A., Reno, P.L. & Rosenman, B.A. (2003) Developmental biology and human evolution*. *Annual Review of Anthropology*, 32, 85–109. Available from: https://doi.org/10.1146/annurev.anthro.32.061002.093223

Ludewig, P.M., Phadke, V., Braman, J.P., Hassett, D.R., Cieminski, C.J. & LaPrade, R.F. (2009) Motion of the shoulder complex during multiplanar humeral elevation. *JBJS*, 91, 378. Available from: https://doi.org/10.2106/JBJS.G.01483

Lukova, A., Dunmore, C.J., Tsegai, Z.J., Bachmann, S., Synek, A. & Skinner, M.M. (2024) Technical note: does scan resolution or downsampling impact the analysis of trabecular bone architecture? *American Journal of Biological Anthropology*, 185, e25023. Available from: https://doi.org/10.1002/ajpa.25023

Lulic-Kuryllo, T., Negro, F., Jiang, N. & Dickerson, C.R. (2021) Standard bipolar surface EMG estimations mischaracterize pectoralis major activity in commonly performed tasks. *Journal of Electromyography and Kinesiology*, 56, 102509. Available from: https://doi.org/10.1016/j.jelekin.2020.102509

Marzke, M.W. (1983) Joint functions and grips of the Australopithecus afarensis hand, with special reference to the region of the capitate. *Journal of Human Evolution*, 12, 197–211. Available from: https://doi.org/10.1016/S0047-2484(83)80025-6

Michilsens, F., Vereecke, E.E., D'Août, K. & Aerts, P. (2009) Functional anatomy of the gibbon forelimb: adaptations to a brachiating lifestyle. *Journal of Anatomy*, 215, 335–354. Available from: https://doi.org/10.1111/j.1469-7580.2009.01109.x

Myers, J.B., Laudner, K.G., Pasquale, M.R., Bradley, J.P. & Lephart, S.M. (2005) Scapular position and orientation in throwing athletes. *The American Journal of Sports Medicine*, 33, 263–271. Available from: https://doi.org/10.1177/0363546504268138

Niskanen, M. & Junno, J.-A. (2009) Estimation of African apes' body size from postcranial dimensions. *Primates*, 50, 211–220. Available from: https://doi.org/10.1007/s10329-009-0131-8

Oki, S., Matsumura, N., Iwamoto, W., Ikegami, H., Kiriyama, Y., Nakamura, T. et al. (2012) The function of the acromioclavicular and coracoclavicular ligaments in shoulder motion: a whole-cadaver study. *The American Journal of Sports Medicine*, 40, 2617–2626. Available from: https://doi.org/10.1177/0363546512458571

Parfitt, A.M. (2002) Misconceptions (2): turnover is always higher in cancellous than in cortical bone. *Bone*, 30, 807–809. Available from: https://doi.org/10.1016/S8756-3282(02)00735-4

Pattin, C.A., Caler, W.E. & Carter, D.R. (1996) Cyclic mechanical property degradation during fatigue loading of cortical bone. *Journal of Biomechanics*, 29, 69–79. Available from: https://doi.org/10.1016/0021-9290(94)00156-1

Pitfield, R., Miszkiewicz, J.J. & Mahoney, P. (2017) Cortical histomorphometry of the human Humerus during ontogeny. *Calcified Tissue International*, 101, 148–158. Available from: https://doi.org/10.1007/s00223-017-0268-1

Plasse, M., Amson, E., Bardin, J., Grimal, Q. & Germain, D. (2019) Trabecular architecture in the humeral metaphyses of non-avian reptiles (Crocodylia, Squamata and testudines): lifestyle, allometry and phylogeny. *Journal of Morphology*, 280, 982–998. Available from: https://doi.org/10.1002/jmor.20996

Preuschoft, H., Hohn, B., Scherf, H., Schmidt, M., Krause, C. & Witzel, U. (2010) Functional analysis of the primate shoulder. *International Journal of Primatology*, 31, 301–320. Available from: https://doi.org/10.1007/s10764-010-9399-1

R Core Team. (2023) R: A Language and Environment for Statistical Computing.

Rabey, K.N., Green, D.J., Taylor, A.B., Begun, D.R., Richmond, B.G. & McFarlin, S.C. (2015) Locomotor activity influences muscle architecture and bone growth but not muscle attachment site morphology. *Journal of Human Evolution*, 78, 91–102. Available from: https://doi.org/10.1016/j.jhevol.2014.10.010

Rein, T.R. (2019) A geometric morphometric examination of hominoid third metacarpal shape and its implications for inferring the precursor to terrestrial bipedalism. *The Anatomical Record*, 302, 983–998. Available from: https://doi.org/10.1002/ar.23985

Roach, N.T. & Lieberman, D.E. (2014) Upper body contributions to power generation during rapid, overhand throwing in humans. *The Journal of Experimental Biology*, 217, 2139–2149. Available from: https://doi.org/10.1242/jeb.103275

Roberts, D. (1974) 6 – Structure and function of the primate scapula. In: Jenkins, F.A. (Ed.) *Primate locomotion*. Academic Press, pp. 171–200. Available from: https://doi.org/10.1016/B978-0-12-384050-9.50011-8. isbn:9780123840509. (https://www.sciencedirect.com/science/article/pii/B9780123840509500118)

Rubin, C., Turner, A., Mallinckrodt, C., Jerome, C., McLeod, K. & Bain, S. (2002) Mechanical strain, induced noninvasively in the high-frequency domain, is anabolic to cancellous bone, but not cortical bone. *Bone*, 30, 445–452.

Rubin, C., Turner, A.S., Bain, S., Mallinckrodt, C. & McLeod, K. (2001) Low mechanical signals strengthen long bones. *Nature*, 412, 603–604.

Ruff, C., Holt, B. & Trinkaus, E. (2006) Who's afraid of the big bad Wolff?: "Wolff's law" and bone functional adaptation. *American Journal of Physical Anthropology*, 129, 484–498. Available from: https://doi.org/10.1002/ajpa.20371

Ruff, C.B. (2006) Gracilization of the modern human skeleton: the latent strength in our slender bones teaches lessons about human lives, current and past. *American Scientist*, 94, 508–514.

Ruff, C.B. & Runestad, J.A. (1992) Primate Limb Bone Structural Adaptations. *Annual Review of Anthropology*, 21, 407–433.

Ryan, T.M. & Shaw, C.N. (2012) Unique suites of trabecular bone features characterize locomotor behavior in human and non-human anthropoid primates. *PLoS One*, 7, e41037. Available from: https://doi.org/10.1371/journal.pone.0041037

Ryan, T.M. & Shaw, C.N. (2013) Trabecular bone microstructure scales allometrically in the primate humerus and femur. *Proceedings of the Royal Society B*, 280, 20130172. Available from: https://doi.org/10.1098/rspb.2013.0172

Ryan, T.M. & Shaw, C.N. (2015) Gracility of the modern Homo sapiens skeleton is the result of decreased biomechanical loading. *Proceedings of the National Academy of Sciences*, 112, 372–377. Available from: https://doi.org/10.1073/pnas.1418646112

Ryan, T.M., Stephens, N., Doershuk, L.J., Saers, J.P.P., Jashashvili, T., Carlson, K.J. et al. (2019) Trabecular bone structural variation in the human postcranial skeleton. *The FASEB Journal*, 33, 19.2. Available from: https://doi.org/10.1096/fasebj.2019.33.1_supplement.19.2

Saers, J.P.P., Cazorla-Bak, Y., Shaw, C.N., Stock, J.T. & Ryan, T.M. (2016) Trabecular bone structural variation throughout the human lower limb. *Journal of Human Evolution*, 97, 97–108. Available from: https://doi.org/10.1016/j.jhevol.2016.05.012

Schlecht, S.H. (2012) Understanding entheses: bridging the gap between clinical and anthropological perspectives. *The Anatomical Record*, 295, 1239–1251. Available from: https://doi.org/10.1002/ar.22516

Schulte, F.A., Ruffoni, D., Lambers, F.M., Christen, D., Webster, D.J., Kuhn, G. et al. (2013) Local mechanical stimuli regulate bone formation and resorption in mice at the tissue level. *PLoS One*, 8, e62172. Available from: https://doi.org/10.1371/journal.pone.0062172

Schwartz, R., Farrell, H.N. & Alemseged, Z. (2024) Trabecular bone response variation in the hominoid clavicle. *CJHB*, 2, 95–99.

Sheikhzadeh, A., Yoon, J., Pinto, V.J. & Kwon, Y.W. (2008) Three-dimensional motion of the scapula and shoulder during activities of daily living. *Journal of Shoulder and Elbow Surgery*, 17, 936–942. Available from: https://doi.org/10.1016/j.jse.2008.04.008

Skinner, M.M., Stephens, N.B., Tsegai, Z.J., Foote, A.C., Nguyen, N.H., Gross, T. et al. (2015) Human-like hand use in Australopithecus africanus. *Science*, 347, 395–399. Available from: https://doi.org/10.1126/science.1261735

Smith, B.H., Crummett, T.L. & Brandt, K.L. (1994) Ages of eruption of primate teeth: a compendium for aging individuals and comparing life histories. *American Journal of Physical Anthropology*, 37, 177–231. Available from: https://doi.org/10.1002/ajpa.1330370608

Smith, S.M., Heaney, L.R. & Angielczyk, K.D. (2024) Small skeletons show size-specific scaling: an exploration of allometry in the mammalian lumbar spine. *Proceedings of the Royal Society B: Biological Sciences*, 291, 20232868. Available from: https://doi.org/10.1098/rspb.2023.2868

Squyres, N. & DeLeon, V.B. (2015) Clavicular curvature and locomotion in anthropoid primates: a 3D geometric morphometric analysis. *American Journal of Physical Anthropology*, 158, 257–268. Available from: https://doi.org/10.1002/ajpa.22785

Stauber, M., Rapillard, L., van Lenthe, G.H., Zysset, P. & Müller, R. (2006) Importance of individual rods and plates in the assessment of bone quality and their contribution to bone stiffness. *Journal of Bone and Mineral Research*, 21, 586–595.

Stern, J.T., Wells, J.P., Jungers, W.L., Vangor, A.K. & Fleagle, J.G. (1980) An electromyographic study of the pectoralis major in Atelines and Hylobates, with special reference to the evolution of a pars clavicularis. *American Journal of Physical Anthropology*, 52, 13–25. Available from: https://doi.org/10.1002/ajpa.1330520104

Susman, R.L., Jack, T., Stern, J. & Jungers, W.L. (1984) Arboreality and bipedality in the Hadar hominids. *FPR*, 43, 113–156. Available from: https://doi.org/10.1159/000156176

Swartz, S.M., Parker, A. & Huo, C. (1998) Theoretical and empirical scaling patterns and topological homology in bone trabeculae. *Journal of Experimental Biology*, 201, 573–590.

Swindler, D.R. & Wood, C.D. (1973) Theoretical and empirical scaling patterns and topological homology in bone trabeculae. In: *An atlas of primate gross anatomy: baboon, chimpanzee, and man*, Vol. 201. Seattle: University of Washington Press, pp. 573–590.

Teece, R.M., Lunden, J.B., Lloyd, A.S., Kaiser, A.P., Cieminski, C.J. & Ludewig, P.M. (2008) Three-dimensional acromioclavicular joint motions during elevation of the arm. *Journal of Orthopaedic & Sports Physical Therapy*, 38, 181–190. Available from: https://doi.org/10.2519/jospt.2008.2386

Thorpe, S.K.S., Holder, R.L. & Crompton, R.H. (2007) Origin of human bipedalism as an adaptation for locomotion on flexible branches. *Science*, 316, 1328–1331. Available from: https://doi.org/10.1126/science.1140799

Tsegai, Z.J., Kivell, T.L., Gross, T., Nguyen, N.H., Pahr, D.H., Smaers, J.B. et al. (2013) Trabecular bone structure correlates with hand

posture and use in hominoids. *PLoS One*, 8, e78781. Available from: https://doi.org/10.1371/journal.pone.0078781

Tsegai, Z.J., Skinner, M.M., Pahr, D.H., Hublin, J.-J. & Kivell, T.L. (2018) Systemic patterns of trabecular bone across the human and chimpanzee skeleton. *Journal of Anatomy*, 232, 641–656. Available from: https://doi.org/10.1111/joa.12776

Velasquez Garcia, A., Salamé, F. & Mura, J. (2023) The stress and strain pattern in the ligaments of the acromioclavicular joint using a quasi-static model. *Clinical Biomechanics*, 101, 105859. Available from: https://doi.org/10.1016/j.clinbiomech.2022.105859

Visualizations Sciences Group. (2017) Avizo Lite.

Voisin, J.-L. (2006) Clavicle, a neglected bone: morphology and relation to arm movements and shoulder architecture in primates. *The Anatomical Record Part A: Discoveries in Molecular, Cellular, and Evolutionary Biology*, 288A, 944–953. Available from: https://doi.org/10.1002/ar.a.20354

Wallace, I.J., Demes, B. & Judex, S. (2017) Ontogenetic and genetic influences on bone's responsiveness to mechanical signals. In: Percival, C.J. & Richtsmeier, J.T. (Eds.) *Building bones: bone formation and development in anthropology*. Cambridge, UK: Cambridge University Press, pp. 233–253.

Wallace, I.J., Judex, S. & Demes, B. (2015) Effects of load-bearing exercise on skeletal structure and mechanics differ between outbred populations of mice. *Bone*, 72, 1–8. Available from: https://doi.org/10.1016/j.bone.2014.11.013

Wallace, I.J., Pagnotti, G.M., Rubin-Sigler, J., Naeher, M., Copes, L.E., Judex, S. et al. (2015) Focal enhancement of the skeleton to exercise correlates with responsivity of bone marrow mesenchymal stem cells rather than peak external forces. *Journal of Experimental Biology*, 218, 3002–3009. Available from: https://doi.org/10.1242/jeb.118729

Wallace, I.J., Tommasini, S.M., Judex, S., Garland, T., Jr. & Demes, B. (2012) Genetic variations and physical activity as determinants of limb bone morphology: an experimental approach using a mouse model. *American Journal of Physical Anthropology*, 148, 24–35. Available from: https://doi.org/10.1002/ajpa.22028

Wallace, I.J., Winchester, J.M., Su, A., Boyer, D.M. & Konow, N. (2017) Physical activity alters limb bone structure but not entheseal morphology. *Journal of Human Evolution*, 107, 14–18. Available from: https://doi.org/10.1016/j.jhevol.2017.02.001

Wang, X., Nyman, J., Dong, X., Leng, H. & Reyes, M. (2022) *Fundamental biomechanics in bone tissue engineering*. Springer Nature.

Ward, C.V. (2002) Interpreting the posture and locomotion of Australopithecus afarensis: where do we stand? *Yearbook of Physical Anthropology*, 45, 185–215. Available from: https://doi.org/10.1002/ajpa.10185

Ward, C.V. (2013) Postural and locomotor adaptations of Australopithecus species. In: Reed, K.E., Fleagle, J.G. & Leakey, R.E. (Eds.) *The paleobiology of Australopithecus*, *vertebrate paleobiology and paleoanthropology*. Dordrecht: Springer Netherlands, pp. 235–245. Available from: https://doi.org/10.1007/978-94-007-5919-0_16

White, T.D., Lovejoy, C.O., Asfaw, B., Carlson, J.P. & Suwa, G. (2015) Neither chimpanzee nor human, Ardipithecus reveals the surprising ancestry of both. *Proceedings of the National Academy of Sciences*, 112, 4877–4884. Available from: https://doi.org/10.1073/pnas.1403659111

Young, N.M., Capellini, T.D., Roach, N.T. & Alemseged, Z. (2015) Fossil hominin shoulders support an African ape-like last common ancestor of humans and chimpanzees. *Proceedings. National Academy of Sciences. United States of America*, 112, 11829–11834. Available from: https://doi.org/10.1073/pnas.1511220112

Zawin, J. & Jaramillo, D. (1993) Conversion of bone marrow in the humerus, sternum, and clavicle: changes with age on MR images. *Radiology*, 188, 159–164.

Zumwalt, A. (2006) The effect of endurance exercise on the morphology of muscle attachment sites. *Journal of Experimental Biology*, 209, 444–454. Available from: https://doi.org/10.1242/jeb.02028

SUPPORTING INFORMATION

Additional supporting information can be found online in the Supporting Information section at the end of this article.

How to cite this article: Farrell, H.N., Schwartz, R., Tsegai, Z.J. & Alemseged, Z. (2025) Locomotor signals in the trabecular structure of the hominoid clavicle. *Journal of Anatomy*, 00, 1–20. Available from: https://doi.org/10.1111/joa.14243